



# Thermal stability of natural fibers and their polymer composites

Mohammad Asim<sup>1</sup> · Mohd T. Paridah<sup>1</sup> · M. Chandrasekar<sup>2</sup> · Rao M. Shahroze<sup>3</sup> · Mohammad Jawaaid<sup>1</sup> · Mohammed Nasir<sup>4</sup> · Ramengmawii Siakeng<sup>5</sup>

Received: 28 October 2019 / Accepted: 5 May 2020 / Published online: 21 May 2020

© Iran Polymer and Petrochemical Institute 2020

## Abstract

Natural fiber-based composites are applied in many structural engineered products from civil constructions to automobile manufacturing due to the properties such as low density, high aspect ratio, biodegradability and ease to work. During the past decades such composites have been thoroughly studied for their mechanical properties and failure behavior and their properties compared with those of synthetic fiber-based composites. Other properties, such as the thermal behavior of natural fibers and composites, have also been studied because they determine the performance of their products possible. It deals with the effect of temperature on adhesive curing, effect of high temperature and fire damage during fabrication. Further, the thermal properties have equal importance in structural applications such as temperature transfer from end to end, load capacity at specific temperature, material behavior and dimensional stability at high temperature. In this respect the isothermal and non-isothermal thermogravimetric analyses are discussed and the importance of glass transition temperature is studied during preparation of composites to ensure their ultimate properties. Although there are several works that have been done on thermal behavior, especially thermogravimetric analysis of natural fibers and their composites, there is no review article available specially focused on natural fiber-based composites, hybrid composites, and nanocomposites. The aim of this review was to focus on the advances in the comprehension of thermogravimetric behavior of natural fibers and compare the effect of natural fibers as reinforced materials in polymer composites.

**Keywords** Thermogravimetric analysis · Natural fibers · Hybrid composites · Biopolymers · Nanocomposites

## Introduction

Natural fibers are characterized as biodegradable, recyclable, and lignocellulosic fibers; however, recent studies have identified them as the best alternative to credible economics and natural protection [1]. Lignocellulosic fibers have many inherent advantages like non-abrasive nature, low energy consumption, high aspect ratio, low density, low cost, and biodegradability as compared to synthetic fibers [2–4]. Although the synthetic reinforced polymer composites possess higher mechanical properties in comparison to the natural fiber, they have a major limitation of being an environmental pollutant and non-biodegradable material [5].

The advance application of composites is based on the detail study of high specific strength-to-weight and specific stiffness-to-weight ratios of composite [6]. Apart from these specific properties such as mechanical, physical, thermal and electrical properties [7], other fundamental aspects need to be focused is life cycle assessment of the products. Further, the environmental concerns of their production are aimed to

✉ Mohammad Jawaaid  
jawaaid\_md@yahoo.co.in

✉ Mohammed Nasir  
mnknasir@gmail.com

<sup>1</sup> Institute of Tropical Forestry and Forest Products (INTROP), Universiti Putra Malaysia (UPM), 43400 Serdang, Selangor, Malaysia

<sup>2</sup> School of Aeronautical Sciences, Hindustan Institute of Technology and Science, Padur, Kelambakkam, Chennai 603103, India

<sup>3</sup> Department of Aerospace Engineering, Universiti Putra Malaysia, 43400 Serdang, Selangor, Malaysia

<sup>4</sup> Forest Products Utilization, College of Forestry, Banda University of Agriculture and Technology (BUAT), Banda, Uttar Pradesh 210001, India

<sup>5</sup> Department of Mechanical and Process Engineering, The Sirindhorn International Thai German, Graduate School of Engineering (TGGS) King Mongkut's University of Technology North, Bangkok, Thailand

reduce the negative impact. It is also worth studying that the world has moved towards renewable and recycled materials from non-recycled materials [1, 8]. The natural fibers and thermoset matrix are used tremendously in automobile sectors for various light and heavy applications such as door panels, seat backs, headliners, package trays, dashboards, interior parts, etc. [9–11]. The market study on global natural fiber composite materials released by Lucintel [12] estimated the market growth at a compound annual growth rate (CAGR) of 8.2% from 2015 to 2020.

There are several large markets such as European Union (Directive 2000/53/EC) and other major automobile makers which give priority to the bio-based reinforced composites for global sustainability. The automobile industries have very complex and precise structures with more than 40,000 small and big parts of nearly 1000 various materials and 10,000 chemical substances. Among all materials, 75% constitutes metals, 17% materials are plastics and the rest are elastomers and textiles. Commercially, composite materials are very successful in semistructural applications and non-structural (cosmetics) purposes; however, the physical and thermal stability are the major constraints [8]; further, the application of biomaterials is restricted due to its heterogeneous characteristics against the homogeneous and very precise synthetic fibers [13]. These biomaterials can be modified by chemical treatment and bring uniformity in interfacial bonding of fibers and matrix that will ultimately improve the thermal resistance and mechanical properties of composites. Although the surface modification increases the processing cost, it improves the quality of composites that reduces the economical competitiveness of the natural fiber composites [14]. However, the choice of natural fibers is still the subject of extensive research around the world. During the extraction of polymers, some basic properties are studied by researchers and manufacturers on thermoset and thermoplastic behaviors, curing temperature and melting temperature. Virgin polymers usually have singular and specific type of chemical structure, so similar basic properties have been found. But natural fibers are very different

from each other in terms of constituent species; even similar fibers have different compositions due to topography and climate. Therefore, each fiber is required to be studied for its properties as well as its behavior when used as a reinforced material. Natural fibers consist of so many minor chemical compositions which affect their interfacial bonding with polymers.

Thermal properties of natural fiber-reinforced composites are a major constrain in their application. At higher temperatures the fiber components, like cellulose, hemicellulose and lignin, start degrading and the major properties of composite change. The suitability of natural fibers with polymers and high temperature stability have been studied for several decades, though the stability of natural fiber with different types of polymers, two different natural fibers reinforced polymer composites or natural fiber reinforced blended with two different polymers are needed to compile information through comparative studies. This study helps researchers select reinforced materials and matrices for the required thermal stability.

A full study is needed to understand the thermal effects on natural fibers and their composites. So far, no studies have reported on the thermogravimetric analysis of natural fibers and their composites. This study is motivated to compile all previous research work on the effect of temperature and its effect on fiber weight loss and its characteristics.

## Natural fiber

Natural fiber is an organic complex material, composed of three major constituents, i.e., cellulose, hemicellulose lignin and some minor components like extractives. Table 1 lists some major agriculture crops and their respective chemical compositions. When the temperature is applied, it results in a variety of physical and chemical changes that ultimately determine the property.

The natural fibers such as water hyacinth, reed (*Phragmites vulgaris*), roselle and sisal (*Agave sisalana* Perr.)

**Table 1** Chemical properties of cellulose-based natural fibers [174, 175]

Fibers	Cellulose	Lignin	Hemicellulose	Pectin	Ash	Moisture content	Wax
Flax	71	2.2	18.6–20.6	2.3	–	8–12	1.5–3.3
Kenaf	31–72	15–19	21.5–23	–	2–5	–	–
Jute	45–71.5	12–26	13.6–21	0.2	0.5–2	12.5–13.7	0.5
Hemp	57–77	3.7–13	14–22.4	0.9	0.8	6.2–12	0.8
Ramie	68.6–91	0.6–0.7	5–16.7	1.9	–	7.5–17	0.3
Kenaf	37–72	15–21	18–24	–	2–4	–	–
CissusquadrAngularis	77.17	10.45	11.02	–	–	7.3	0.14
Abaca	56–63	7–9	15–17	–	3	5–10	–
Sisal	47–78	7–11	10–24	10	0.6–1	10–22	2
Henequen	77.6	13.1	4–8	–	–	–	–

differ in their decomposition temperature ( $T_d$ ). To evaluate the behavior of thermal degradation, the temperature range was examined between 290 and 490 °C [15]. Initial weight loss was recorded in the temperature range between 50 and 100 °C due to evaporation of water molecules. Further weight loss was found in the temperature range of 200–350 °C due to the degradation of hemicelluloses, though thermal degradability of lignin and hemicellulose were in the temperature range of 300–450 °C and 200–300 °C, respectively. Due to hemicellulose and lignin, approximately 60% of the thermal decomposition of natural fibers occurred in the temperature range of 230 and 350 °C [16]. The initial decomposition of the components may explain the lower thermal stability [15]; however, oxidative decomposition, characterized by rapid weight loss at higher temperatures, is more consistent with thermal stability [17]. Table 2 gives a detailed description of thermal degradation of various natural fibers at different temperatures.

**Table 2** DTG data of biomass samples [176] (with permission)

Fibers	First-stage		Second-stage	
	$T_{\text{peak}}$ (°C)	Temperature range (°C)	$T_{\text{peak}}$ (°C)	Temperature range (°C)
Cellulose	338	300–360	—	—
Lignin	—	—	548	450–600
Almond shell	298	250–390	477	400–720
Briquette	343	260–400	509	410–550
Cocoa bean husk	312	225–350	627	425–634
Coffee bean husk	319	220–360	502	440–520
Corn cob	289	250–340	454	400–550
Pineapple leaf	344	250–380	496	420–570
Rice husk	334	260–360	450	400–540
Sainfoin	301	230–330	456	390–522
Scrubland pruning	334	260–370	538	400–760
Thistle	345	240–400	473	420–550
Wheat straw	312	260–360	543	420–650

The thermogravimetric behavior of natural fibers directly depends on their chemical constituents. Similar natural fibers such as jute, sisal, wood and cotton have similar TG/DTG curves and thermal decomposition pattern. Table 3 shows three stages of weight loss associated with the TG curve. The first stage explains the evaporation of moisture content at lower temperature, the second stage is decomposition of hemicellulose at medium temperature and the final stage illustrates the decomposition of lignin and cellulose at higher temperature. Sometimes the first stage does not appear due to very low moisture content or minimum weight loss and exhibits the second stage as the first stage [18, 19]. Some researchers [13, 19] have considered the evaporation of moisture content to 200 °C as initial weight loss which corresponds to a maximum weight loss of 10%. The second stage of degradation shows the loss of weight of more than 70% of initial weight at temperature of about 500 °C. The third stage represents the end of thermal degradation and makes sure that all the components of natural fibers are thermally degraded at temperature around 800 °C and the final remaining mass reaches 20% of the initial weight as ash and char content.

The corresponding TGA curves revealed the contribution of fibers' constituents in thermal degradation and showed the highest rate of thermal decomposition peaks. Figure 1b shows thermal decomposition of different natural fibers that reflects the different decomposition rate at different fiber constituent ratio.

According to Monteiro et al. [13], less than 100 °C caused an initial decrease in total weight percentage and the DTG peak indicates the availability of OH group in fiber cells. The thermal degradation of the major fiber composition (cellulose, hemicellulose and lignin) of natural fibers starts from the next stage. In the second stage, the curve of DTG reveals the decomposition of cellulose. In the stretch of the peak it is described that the initial decomposition is due to hemicellulose while the end portion shows lignin degradation. The third stage shows the char and other material decomposition reactions [20]. Natural fibers affect TGA results that work

**Table 3** Stages of thermal degradation of natural fibers

Stage 1	Stage 2	Stage 3	References
50–100 °C: Evaporation of moisture in the fibers degradation	200–300 °C: Decomposition of hemicelluloses	400–500 °C: Weight loss due to lignin and cellulose	[15]
50–50 °C: Attributed to the release of water absorbed by the fibers	250–370 °C: Depolymerization of the hemicellulose and the cleavage of glycosidic linkages of cellulose	340–370 °C: Assigned to the degradation of $\alpha$ -cellulose	[173]
60–100 °C: corresponds to vaporization of water molecules	282–306 °C: thermal decomposition of hemicellulose, lignin, pectin and the glycosidic linkages of cellulose	388.7–448 °C: Degradation of $\alpha$ -cellulose	[52]
	270–330 °C: Associated with the degradation of hemicelluloses and pectins	448–472 °C: Corresponds to the degradation of cellulose and lignins	[19]

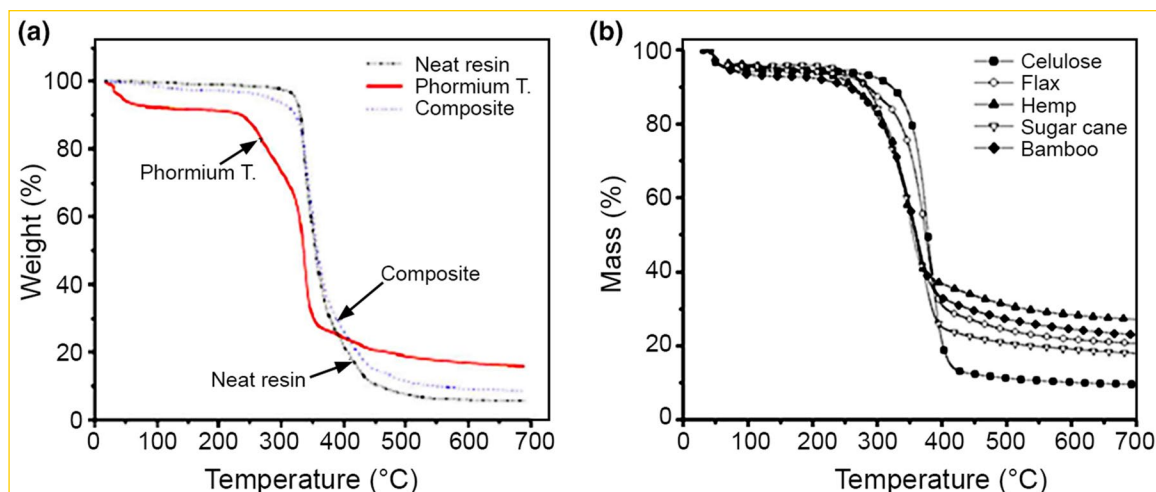


**Fig. 1** TGA curves of different natural fiber polymers and their composites [42, 173]

under different inert conditions (helium and nitrogen) or oxidative (air and oxygen) conditions [13].

In another study, the thermal behavior of jute fiber was studied for untreated and alkali-treated jute fibers and different peaks of untreated and treated fibers were observed [21]. The untreated fibers revealed two peaks: the first peak represented the degradation of hemicellulose and glycosidic union de-polymerization at 300 °C and the second peak which was recorded at 365 °C showed the thermal degradation of cellulosic content. Since cellulose contributes the major portion of natural fiber, the second peaks play a great role in weight loss. The broad peak in all the range represents the presence of lignin [21]. In alkali-treated fiber, unlike untreated fiber, there was only one peak that appeared at lower temperature compared to the second peak of untreated fiber. The first peak did not appear in treated fibers due to partial removal of lignin and hemicelluloses. The further degradation of complex structure of lignin and hemicellulose was revealed, but at the lower temperature of the second peak when compared to untreated fibers [22].

The thermal properties of the agave fiber were investigated and the initial mass loss of 5% was observed at 221 °C, and in the second thermal degradation, a major weight loss at 379 °C was achieved with a 64% reduction in mass [23]. Furthermore, the measured remaining residue of total mass was only 14% and was found at about 990.5 °C. The thermal properties of the agave fibers revealed the sustainability of temperature up to 221 °C which can be utilized easily where the maximum temperature is less than 221 °C. Some works reported that natural fibers were incorporated in polymers as reinforcement and studied the main stages of weight loss due to reinforcement and effect on the thermal stability of composites. Through TGA, the thermal degradation process of composites can be studied and the obtained parameters determine the degree of degradation of materials [24]. Yao

et al. [16] studied the degradation temperature of different natural fibers for comparative study. The thermal properties affect the morphology of natural fiber-reinforced composites significantly. Depending on the temperature, the composites expand or contract, creating cracks in the composites that eventually retain moisture. The natural fibers take up moisture through capillary action, causing thickness swelling in composites [25]. Cellulose-reinforced polyethylene composites were used to pass through the oxidation process which improved the interfacial bonding of cellulose and matrix and also had a positive effect on thermal degradation [26]. Another experiment on untreated and silane-treated sisal fibers was done, and degradation temperature and mass loss were calculated [27]. The mass loss of 5%, 10%, and 50% was recorded at 83, 255, and 360 °C for untreated fiber, and at 100, 278, and 365 °C for saline-treated fiber, in the stated order. The hemicellulose of sisal fibers was thermally degraded at 297 °C and cellulosic content was degraded as revealed in the second stage at 365 °C.

## Thermogravimetric analysis (TGA)

Thermogravimetric analysis (TGA) is a standard method to study the overall thermal stability of natural fibers. In this method, the thermal degradation of natural fiber composites with increasing the temperature is studied along with numerical calculation of quality degradation. When the temperature increases, the weight of the fiber drops slowly and at the point of glass transition weight drops sharply over a narrow range and finally turns back to zero slopes as the reactant is exhausted. The degradation process in TGA can be presented in the curve, which is dependent on the kinetic parameters of the pyrolysis such as frequency factor, reaction order, and activation energy. The value obtained in the

curve depends upon various factors such as sample mass, sample shape, atmosphere, flow rate, heating rate, and the mathematical treatment applied.

The differential thermal analysis (DTA) represents the reaction of heat with the sample and the reaction percentage per min is indicated by the deflection or peak. In a single-factor experiment, if the temperature of reaction varies, the peak varies in respect to temperature as well as energy of activation. The difference in peak temperature determines the activation energy for the reactions with different reaction orders [28]. In thermal degradation, the thermogravimetric analysis (TGA) and derivative thermogravimetric (DTG) curves determine the weight loss and identify the decomposition of material at a certain temperature, respectively [26].

### Isothermal and non-isothermal thermogravimetric analysis

TGA is known for the thermal degradation of material with respect to temperature and time, and for determining the final residue to analyze the thermal stability. In isothermal technique the temperature in furnace is constant and degradation or decomposition of mass is measured with time. In non-isothermal technique the temperature in furnace increases with time in a linear manner. In non-isothermal technique, the heating rate is constant and weight loss is measured with respect to time and temperature and a mass versus temperature or mass versus time curve is developed. Isothermal and non-isothermal techniques differ in the assumption of properties and process of data collections. This difference in data, due to its specific method, provides completely different information.

The isothermal kinetic study predicted the thermal decomposition of hemicellulose, cellulose, lignin, and xylan [29]. The thermogravimetric analysis used five torrefaction temperatures of 200, 225, 250, 275, and 300 °C for 1-h span to study the recommendation value for the reaction of hemicellulose, cellulose, lignin and xylan shown in Fig. 2. The activation energy of hemicellulose, cellulose, lignin and xylan is 187.06, 124.42, 37.58 and 67.83 kJ/mol, respectively.

The non-isothermal method is used for the pyrolysis experiments which help to study relation of mass loss verses time. The method also helps to determine the activation energy which provides different results. However, the isothermal process of thermal degradation is used for plotting natural log of reaction coefficient against the inverse of temperature. In this plotted reduction method, the kinetic parameters are obtained from the slope and intercept of the resulting linearized equation.

The data of non-isothermal experimentare are also used to plot an equation in a linearized manner, where the straight line represents the activation energy and reaction order. Isothermal and non-isothermal methods need different data to study the kinetic parameters [30]. Instead of error, single-heating-rate methods or non-isothermal method is very popular for analyzing the solid-state kinetics. There are various ways to study single-heating-rate methods such as Coats–Redfern method, MacCallum–Tanner equation, Madhusudana–Krishnan–Ninan equation, Horowitz–Metzger equation, Van Krevelen method, etc. [31].

### Coats–Redfern equation

The Coats–Redfern equation (Eq. 1) has some disadvantages in calculation of activation energy and pre-exponential

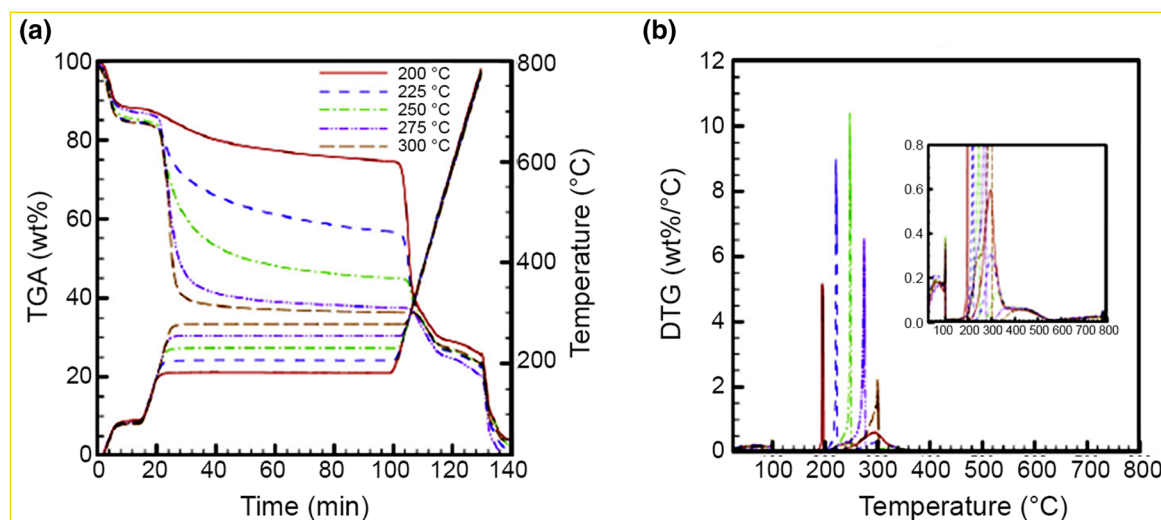


**Fig. 2** Distributions of **a** TGA and **b** DTG of natural fiber at five different torrefaction temperatures [29]



factor, which cannot be done without pre-assumption of the reaction model. It is recommended that you assume the initial value of the reaction order is “ $n$ ” and find the correct value of the kinetic parameters until the best straight line is obtained, or the error is less than the tolerance value.

$$\ln \left[ \frac{g(\alpha)}{T^2} \right] = \ln \left[ \left( \frac{AR}{\beta E} \right) \left( 1 - \frac{2RT}{E} \right) \right] - \frac{E}{RT}. \quad (1)$$

Since  $\frac{2RT}{E} \ll 1$  in the temperature range usually employed, the term  $\ln \left[ \left( \frac{AR}{\beta E} \right) \left( 1 - \frac{2RT}{E} \right) \right]$  in Eq. (1) is assumed to be sensibly constant. Thus, the slope of the plot of  $\ln \left[ \frac{g(\alpha)}{T^2} \right]$  versus  $\left( -\frac{1}{RT} \right)$  will be equal to  $E$ , and the value of pre-exponential factor can be calculated by equating the intercept of the equation equal to  $\left[ \left( \frac{AR}{\beta E} \right) \right]$ . These reaction models can cause different kinetic parameters with the same experimental data. The resulting curve for the relevant data from each assumed model shows the amount of activation energy.

### Horowitz–Metzger equation

$$\ln g(\alpha) = \left( \frac{ART_s^2}{\beta E} \right) - \frac{E}{RT_s} + \frac{E\theta}{RT_s^2}. \quad (2)$$

Activation energy values can be calculated from the plot of  $\ln g(\alpha)$  versus  $\theta$ , whose slope will be equal to  $\frac{E}{RT_s}$ . The major disadvantage of this method is its dependence on peak temperature,  $T_s$ , whose value depends on the heating rate and sample weight.

### van Krevelen equation

$$\ln = \left[ \frac{1 - (1 - \alpha)^{1-n}}{1 - n} \right] = \ln = \left[ \frac{A}{\beta} \left( \frac{0.368}{T_s} \right)^{\frac{E}{RT_s}} \left( \frac{E}{RT_s} \right)^{-1} \right] + \left( \frac{E}{RT_s} + 1 \right) \ln T. \quad (3)$$

The values of activation  $E$  and  $A$  can be calculated from the slope and intercept of the plot of  $\ln \left[ \frac{1 - (1 - \alpha)^{1-n}}{1 - n} \right]$  versus  $\ln T$  respectively.

By applying the equation of van Krevelen and Hofzyer method (Eq. 4) [32, 33] limiting oxygen index (LOI) can be calculated by char residue obtained from TGA testing. Ferdosian et al. [33] studied the LOI by using data of TGA of bisphenol-based epoxy and epoxy composites comprising diglycidyl ether of bisphenol A (DGEBA)-based epoxy resin and various percentages of lignin-based epoxy. In this research TGA testing was investigated at heating rate  $10^\circ\text{C}/\text{min}$  and temperature range from room temperature to  $800^\circ\text{C}$ . LOI is fire resistance testing, which helps to study

the minimum amount of oxygen required to initiate the combustion of materials. It is one of the important tests to grade products according to the topography (presence of oxygen in atmosphere, mountainous areas have less oxygen content). This test is widely used in polymer composites and its effects on fire retardancy [34]:

$$\text{LOI} = 17.5 + 0.4\text{CR}, \quad (4)$$

where CR represents the char residue obtained from the TGA results.

LOI can be calculated by putting char content in Eq. (4). According to the standard, below 20.95% is considered as easily flammable; however, LOI above 28% is considered as “self-extinguishing” materials [34].

Another simple equation of heat resistance index ( $T_s$ ) has been used in research on the synthesis of bio-based epoxy resin from Japanese green tea (*Camellia sinensis*) [35]. Chain of synthesized epoxy was compared with the chain of bisphenol-A (BPA)-derived epoxy by using glass transition ( $T_g$ ) analysis. Thermograph from TGA showed good thermal stability at  $169^\circ\text{C}$  with lower weight loss due to lesser amount of unreacted component. Equation (5) is used to calculate heat thermal resistant temperature of cured resins from the temperature difference at 5% and 30% weight loss ( $T_{d5}$  and  $T_{d30}$ , respectively) obtained from TGA curves.  $T_s$  was determined by using Eq. (5) [36, 37]:

$$T_s = 0.49[T_{d5} + 0.6 \times (T_{d30} - T_{d5})]. \quad (5)$$

The  $T_s$  of 5% and 30% weight loss of the resins cured with lignin were found to be lower than that of resin cured without lignin. It may be due to degradation or epimerization of the catechin compounds during extended periods of heat drying at  $80^\circ\text{C}$ ; consequently, the significant decrease in polyphenol content which is typically observed following heat treatment [38]. This also helps to understand that lignin can be used as a natural curing agent, and usable as a hard segment in epoxy resin network, which increases the glass transition of the resultant polymer network. Therefore, the use of lignin as a curing agent could induce relatively high chain rigidity in the polymer network due to increasing crosslinking [39]. Another research on extraction of phenolic resin from green tea leaves and its use for the production of thermoset epoxy resins showed its high reactivity associated with a high crosslinking density and high thermal resistance [37]. The statistic heat-resistant index temperature ( $T_s$ ) is characteristic of the thermal stability of the cured resins. This value is determined from the temperatures at 5% weight loss ( $T_{d5}$ ) and 30% weight loss ( $T_{d30}$ ) of the sample obtained by thermogravimetric analysis. The statistic heat-resistant index temperature ( $T_s$ ) is calculated by Eq. 5.

## Material selection based on TGA

When preparing new materials, the choice of raw materials, production technique, and final products are equally important. For heavy duty utilization, material should be mechanically strong and thermal stable as well, because heat from mechanical energy can reduce the loading capacity. In this case TGA helps to know the thermal properties of material and also helps to understand the suitability for the material. TGA helps a lot when structural precision is required in products. There are many machine components that are structurally stable after TGA testing. It can be assured at what temperature the material will change its phase or structure.

Some researches based on kenaf fiber and pineapple leaf fiber-reinforced polymer composites have been performed on the thermal properties and found out the  $T_g$ . A research based on kenaf fiber and pineapple leaf fiber-reinforced high-density polyethylene [40] was studied and compared with kenaf fiber and pineapple leaf fiber-reinforced phenolic composites [41] shown in Fig. 3.

From the figure it is shown that initial thermal degradation in both thermographs revealed between 280 and 300 °C, due to degradation of cellulose and hemicellulose. Figure 3b has more fiber content so decomposition at this point must be higher. In Fig. 3a, the polymer showed melting point at 464.9 °C, and after addition natural fibers there is no improvement recorded. On the other hand, Fig. 3b shows very slow thermal degradation for the polymer and final residue is more than 50%. After addition of natural fibers the thermal degradation was decreased but the process was very slow due to the polymer. In conclusion, it is suggested that selection of polymer in composites must be based on its  $T_g$ , where in fact polymer is the key factor of thermal stability in natural fiber-reinforced polymer composites.

## Natural fiber-reinforced composites

### Thermoset composites

Many researchers have studied various natural fiber-reinforced based composites and characterized their properties. Among all those characterizations, the thermal properties of natural fiber-reinforced thermoset polymer composites are one of the critical features, analyzed by using thermogravimetric analysis which is summarized in Table 4.

Thermal behavior of raw fibers of phormium and its reinforced composites was investigated through the TGA technique [42], the thermal degradation reveals two primary phases in the curves shown in Fig. 1a. The initial weight loss in raw fibers of phormium was recorded 8% between 37 °C and 130 °C due to moisture content present in the fiber core. Fiber thermal degradation began between 200 and 305 °C, indicating that thermal degradation was caused by cleavage of cellulose glycosidic bonds and depolymerization of hemicellulose and pectin [43, 44]. The highest thermal degradation of natural fibers was recorded at 305–370 °C due to the degradation of cellulosic content. Degradation temperature of lignin has a wide range between 200 °C and 900 °C due to the complex aromatic structure of lignin with various branches [43–45].

The DTG curve of phormium-reinforced composites was acquired at 347 °C which is the highest among all natural fibers and matrix composite. The thermal degradation temperature of natural fibers and matrix are 337 °C and 347 °C, respectively. Another research based on jute fiber-reinforced vinyl ester composites illustrated that thermal degradation of composites occurs in two steps [22]. The first degradation step indicated the decomposition of natural fibers at 368 °C; however, the second degradation step represented the decomposition of matrix. The thermal degradation of

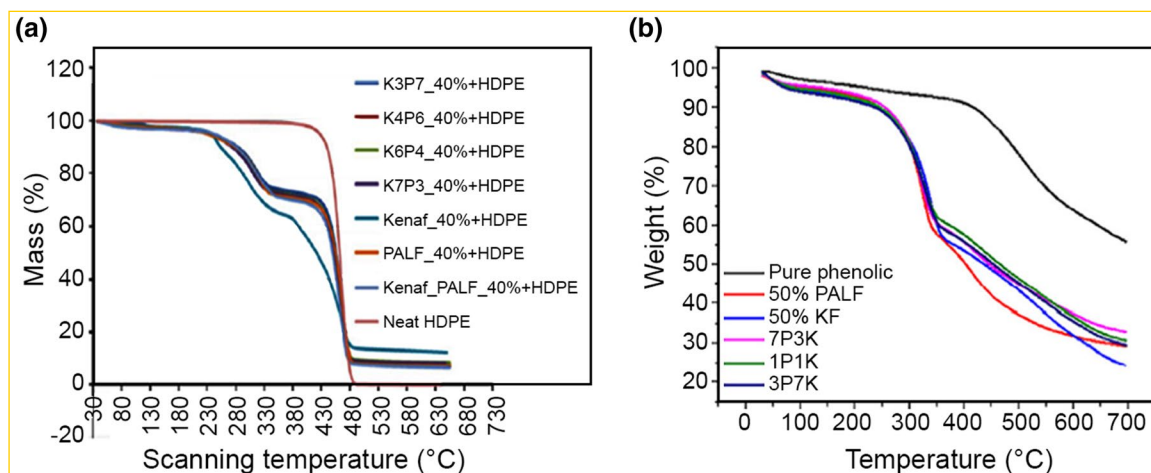


**Fig. 3** Comparative thermographs of polymer composites for similar natural fibers

**Table 4** Works reported on thermogravimetric analysis of natural fiber-reinforced thermoset thermoplastic, and biopolymer-based composites

Reinforcement	Matrix	References
<b>Thermoset polymers</b>		
Phormium tenax leaf fibers	Epoxy resin	[42]
Coconut sheath fiber	Epoxy resin	[46]
Kenaf	Epoxy resin	[177]
	Epoxy resin + phenolic resin	[178]
Cellulosic fibers from eucalyptus wood	Phenolic resin	[179]
Cellulosic fibers from eucalyptus wood	Phenolic foams	[180]
Pine needle	Urea formaldehyde (UF)	[181]
Hemp fiber mats	Unsaturated polyester resin	[182]
Hemp	Unsaturated polyesterresin	[183]
Roselle fiber	Vinyl ester	[184]
Sugar palm fiber	Vinyl ester	[185]
Bleached kraft softwood pulp fibers	Unsaturated polyester and vinyl ester	[186]
<b>Thermoplastic polymers</b>		
Flax, hemp and sisal	Polypropylene	[58]
Pine cone fibers	Polypropylene	[63]
Coir fibers and shell particles	Polypropylene	[187]
Hemp fibers	Polypropylene	[187]
Almond shells particles	Polypropylene	[188]
Almond shells particles	Polypropylene	[189]
Kenaf fiber	Polyurethane	[59]
Roselle fiber	Polyurethane	[190]
Doum fibers ( <i>Chamaerops humilis</i> )	Low-density polyethylene	[62]
<i>Sansevieria cylindrica</i>	Polyester	[191]
<b>Biopolymer</b>		
Sisal fiber	Rubber seed oil-based polyurethane	[77]
Hemp fiber	Phenol-based cashew nut shell liquid (CNSL)	[192]
Sisal fibers	CNSL	[192]
Novel silk	Poly(butylene succinate)	[193]
Jute	Poly(butylene succinate)	[194]
Jute	Poly(lactic acid)	[74]
Kenaf and rise husk	Poly(lactic acid)	[80]
Coir and pineapple leaf fiber	Poly(lactic acid)	[137]

composites was studied at various heating rates and found slight variation. The thermal stability was improved with increasing the heat rate. The comparative study of residual amount of matrix, fiber and composites revealed that the residual amount of composites is in between that of the matrix and fibers.

Thermal properties of treated and untreated coconut sheath fiber-reinforced epoxy composites were studied [46]. Both treated and untreated composites revealed weight loss at the same temperature. The initial weight losses were due to evaporation of hydroxyl groups and further thermal degradation was due to degradation of hemicellulose at 100–105, 230 and 300 °C, respectively. The final thermal degradation was subjected to the degradation of cellulose and epoxy at the temperature of 300–400 °C. The residual amount of treated composites was less than that of the untreated

composites because char yield depends on the availability of lignin in the fibers. It indicated that treatment of natural fibers partially removed lignin and caused the char content to be less than that of the untreated composite [46].

A comparative study of thermal properties of jute and bamboo composites was done and weight loss at various temperature was measured through TGA curves [47]. Initial weight loss near to 100 °C is due to the hydroxyl group presence in jute and bamboo fibers. Both composites were degraded thermally in the temperature range of 240–260 °C. The accurate thermal degradation of jute composite was recorded at 255 °C; however, the bamboo composites were degraded thermally at 246 °C. The higher the thermal degradation temperature of the composite jute, the better its thermal properties than the bamboo epoxy composite. A study based on date palm fiber



(DPF)/epoxy composite at various fiber loadings was done to investigate the thermal properties through TGA analysis [48]. The initial loss in the range of 60–100 °C is an indication of the presence of hydroxyl groups in DPF. Further it was observed that the presence of water molecule in the cell wall structure or void space and the water absorption at the fiber–matrix interfacial bonding [49] indicate the minimizing mechanical strength of natural fiber composites [50]. Further, the fiber loading of 40% DPF and 50% DPF exhibit the thermal degradation at 299.72 °C and 316.9 °C, respectively. However, the final residual percentage of pure epoxy, 40% DPF and 50% DPF was 9.58%, 12.51% and 19.8%, respectively. The residual amounts were increased with increasing the fibers in composites, though 60% fiber loading reduced the residual amount because the matrix was less and could not hold the fibers properly. The thermal properties of DPF composites revealed that their properties are mainly due to the thermal decomposition of hemicellulose, lignin, pectin and the glycosidic linkages of cellulose of natural fibers [51].

Thermal behavior of phenolic resin, untreated and saline-treated PALF and kenaf composites at various fiber loadings was investigated [52]. Kenaf and PALF composites revealed that weight loss below 100 °C corresponds to availability of hydroxyl group in all natural fiber-reinforced composites [18, 53]. Pure matrix did not show weight loss in the beginning and a single-stage thermal degradation was found at 420.73 °C with 32.16% weight loss. The thermal degradation of matrix depends on the dihydroxy phenyl methane units available in the phenolic groups [54]. Untreated PALF and kenaf composites indicated the first stage of thermal degradation at 282–303 °C; however, treated PALF and kenaf composites revealed initial stage of degradation at 293.14 and 305.41 °C, respectively. The initial thermal degradation was initiated due to the presence of several constituents in natural fibers such as glycosidic linkages of cellulose, pectin hemicellulose and lignin [20]; however, thermal depolymerization of hemicellulose and cleavage of the glucosidic linkage of cellulose of treated composites improved the thermal stability [55]. The temperatures of final thermal degradation of PALF-reinforced composites and kenaf-reinforced composites were recorded between 388.7 and 422 °C and 408.58 and 447.99 °C, respectively, because of the thermal degradation of  $\alpha$ -cellulose and depolymerization of matrix [26, 27].

### Thermoplastic polymer composites

There are several works reported on the fabrication process of natural fiber-reinforced thermoplastic composites and their properties such as physical, mechanical, thermal,

electrical conductivity and fire retardancy. Of all the properties, thermal properties are one of the most important for temperature tolerance of composites. The thermogravimetric analysis is one of the test methods used to study natural fiber-reinforced thermoplastic polymer composites, as shown in Table 4.

Pineapple leaf fibers and betel nut husk-reinforced PP hybrid composites were studied at various fiber loadings with equal fiber ratio in hybrid composites [56]. The TGA curve of hybrid composite of all fiber loadings revealed that hydroxyl groups cause initial weight loss below 100 °C. Hybrid composites with 5% and 15% fiber loading revealed that their thermal degradation occurs around 225–358 °C and 223–374 °C, respectively, whereas 10% fiber loading hybrid composite exhibited that its decomposition is around 250–410 °C. In another study the flax/PP composites copolymerized with granulate MAPP of type A were studied by TGA and DTG and it turned out that the thermal degradation was three-stage. The first stage of thermal degradation is due to the presence of water molecules, the second degradation is due to hemicellulose and cellulose and the final stage is due to the presence of lignin [57]. The DTG curves did not show any charring peak at 500 °C. However, the composites showed two distinct peaks in the range of 369.4–374.8 °C and 432.4–481 °C which indicated the rate of thermal degradation of flax and PP, respectively [58]. Another study on kenaf-reinforced thermoplastic polyurethane (TPU) composites showed thermal properties through TGA curves [59]. The initial weight loss was recorded about 9.5% in the temperature range of 31–153 °C, which showed very high moisture content in kenaf fibers. Further mass loss was recorded at 194–330 °C due to the degradation of hemicellulose and cellulose and lastly degradation was due to lignin content at 305–386 °C. The thermal degradation of pure TPU showed a wide range of temperature from 250 to 539 °C. The DTG peak of TPU degradation at 363 °C was due to the polymerization of polyol–isocyanate bond. Once the temperature is reached, the isocyanate is evaporated and condensed again into smoke, but the polyol is the same and decomposed at higher temperatures [60]. It is also observed that increasing the fiber loading in TPU decreased the thermal stability more than that of pure TPU. Thermal degradation of natural fiber-reinforced TPU composites revealed dehydration at initial temperature and showed thermal cleavage of glycosidic linkage by trans-glycosylation and scission of C–O and C–C bonds at low temperatures. Thermal degradation at higher temperature was attributed to the aromatization, involving dehydration reactions [59]. The thermal properties of pure LDPE and natural fiber-reinforced LDPE composites were investigated using TGA [61]. The initial mass loss between 100 and 150 °C showed that fibers have moisture content. Addition of reinforced materials reduced the thermal stability and the doum fibers and LDPE matrix showed high shear

strength and frictional forces which prevented the breaking of LDPE chains that improved mechanical properties [62]. The thermal properties of pinus fibers, PP matrix and pinus fiber-reinforced PP composites were analyzed by TG technique [63]. The pinus fibers showed thermal degradation at two temperatures: the initial thermal degradation was recorded in the range of 220–280 °C due to the degradation of hemicellulose; however, the second stage of thermal degradation was revealed in the range of 280–300 °C due to degradation of lignin and cellulose [64]. After incorporation of pine cone fiber in PP, the degradation temperature decreased from 355 °C for neat PP to 321 °C for a 25 wt% pine cone-reinforced PP. DTG illustrated that compatibilizer affected the thermal stability when compared to fiber/PP composites without compatibilizer. Thermal properties of curaua fiber-reinforced high-density polyethylene composites were studied in the presence of two different coupling agents shown in Fig. 4 [65]. The TGA results of pure HDPE showed less stability than the composites. The other composites containing coupling agent of PE-g-MA showed the least thermal stability. However, with other coupling agent, [poly(ethylene-co-vinyl acetate)] (EVA), it was more stable. The least thermal stability was explained due to better interfacial bonding between the acid groups of the maleic anhydride and the –OH groups on the fiber surfaces. The better interaction may promote degradation process [65].

The thermal degradation of untreated and treated jute/HDPE composites was studied [66]. The complete decomposition of pure HDPE was observed at 430–515 °C. For the 30% fiber loading of jute-reinforced HDPE the initial decomposition was between 304.7 and 382 °C due to dehydration and thermal cleavage of glycosidic linkage by transglycosylation and breakage linkage of C–O and C–C bonds.

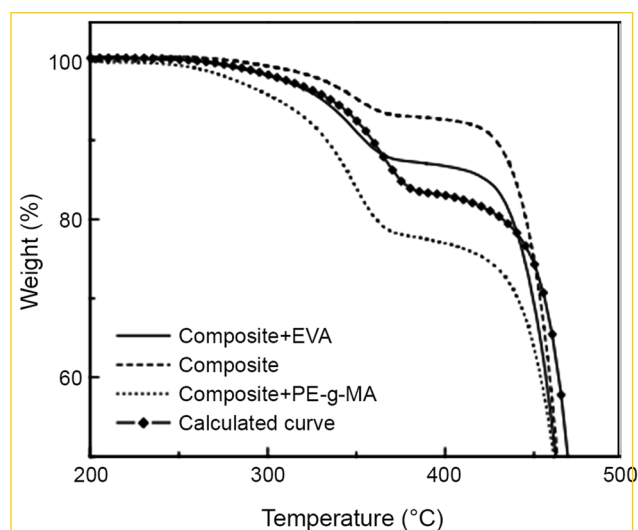


**Fig. 4** Curaua fiber-reinforced high-density polyethylene composites [65] (with permission)

The second thermal degradation was observed between 452 and 530.7 °C due to aromatization. Other researcher also found the same trend for PALF-reinforced HDPE composites [67]. The treated composite was decomposed at 364 °C due to thermal cleavage and scission of C–O and C–C bonds. The major degradation was detected between the range of 479.7 and 598.7 °C which was almost the same as that of the untreated jute/HDPE composite and its char residue was lower than the char residue of untreated composites [66].

### Natural fiber-reinforced biopolymer composites

The annual consumption of polymers are increasing with the rate of 5% and is estimated to be more than 300 million tons [68]. Mostly, the polymers used in industrial production of plastics are extracted from petrochemical resources. Utilization of petrochemical-based polymers in plastic manufacturing is almost 7% of the global oil and gas consumption [69].

These non-degradable synthetic polymers pose a significant threat to the environment and sustainable development. Some initiatives have been taken to develop innovative technologies from renewable feed stocks to biopolymeric materials' processing. Some renewable feed stocks such as natural oils, polysaccharides (starch and sugars), wood (lignocellulose) and proteins are broadly used to extract monomers [70, 71]. Among the renewable feedstocks, triglyceride oils extracted from soybeans are easily available, of relatively low cost and have chemical functionality, as well as 108 million metric tons of soybeans were harvested in USA in 2014 [72, 73].

The thermal properties of jute/PLA composites were studied and weight loss at various temperatures was observed [74]. Jute fibers initially lost their weight near 100 °C due to water molecules present in the cell wall. The second and third thermal degradations were recorded at 280 °C and 360 °C, respectively, due to the decomposition of low molecular weight of hemicellulose, lignin and cellulose [75]. For jute/PLA composites, single-stage thermal degradation has also been recorded at 346 °C. The thermal stability of composite is lower than that of pure PLA, which may be due to the jute fibers. Alkali, permanganate and peroxide treatments of jute fiber reduced the thermal stability of the composites as compared to that of untreated jute fiber/PLA composites. However, silane treatment of jute fiber-reinforced composites improved the thermal properties due to the elimination of easily hydrolyzed substances which usually degrade below the degradation temperature of hemicellulose, lignin and cellulose [74, 76].

A study on sisal/rubber seed oil-based polyurethane (RSOPU) composites showed thermal degradation at three distinct temperatures [77]. The initial weight loss was below 100 °C due to the evaporation of moisture content. The second and third stages of thermal degradation were due

to cellulose, lignin and hemicellulose at 250 and 480 °C, respectively [78]. Three-stage degradation was recorded for thermal degradation of RSOPU. The urethane bonding of polyurethanes was degraded between 217 and 336 °C [79]. However, the final stage of thermal degradation was between 450 and 500 °C due to the degradation of rubber seed oil moiety [77].

The thermal properties of kenaf and rice husk (RH)-reinforced PLA were investigated by TGA and it was found that the initial temperature belongs to moisture evaporation (Fig. 5) [80]. Fiber loading was studied and it was revealed that the addition of natural fiber decreases the temperature of thermal degradation of composites [81]. The highest weight loss of rice husk and kenaf was recorded between 230 °C and 360 °C corresponding to the degradation of the cellulosic substances of hemicelluloses, cellulose and lignin.

Another research on TGA studies of silane-treated and -untreated sisal fibers-reinforced bio-PU composites recorded thermal decomposition and found similar mass degradation curve for both untreated and treated fibers [82]. However, silane-treated composites showed better thermal stability due to better interfacial bonding [27].

A research based on the corn- and rice starch-based bioplastics for packaging applications was done using TGA and identified three stages of degradation: the first temperature range was between 100 and 200 °C and indicated small weight loss due to moisture evaporation; the second stage showed major evaporation between 250 and 300 °C which was due to the decomposition of gelatin and starch, and the third stage showed only char content [83]. The thermal properties of bamboo fiber-reinforced cashew nut shell liquid (CSNL) biocomposites were investigated by TGA and it was found that the first stage of degradation was in the temperature range between 250 and 380 °C due to decomposition of pectin, hemicellulose and cellulose [84]. The second stage

of thermal degradation revealed the degradation of polymers linkages in the range of 400–450 °C. Alkali modified fiber-reinforced composites improved the maximum degradation temperature in the DTG curve from 400 to 421 °C [84]. Thermal degradation of the polymer showed a wide range of decomposition from 250 to 450 °C which was due to several chemical decompositions such as CO, CO<sub>2</sub>, CH<sub>4</sub>, phenols and cresols [85].

Thermal stability of natural fiber-reinforced CNSL composites was investigated and there was no weight loss below 100 °C which was due to hydrophobic nature of CSNL [86]. The treated composites showed weight loss below 100 °C and treated composite with higher concentration of NaOH showed higher weight loss below 100 °C because alkaline treatment exposed the hydroxyl groups of the fiber and so increased their interaction with water [87]. The DTG curves clearly revealed the first peak which was due to evaporation of moisture and the second peak which was due to the degradation of primary constituents of natural fibers [88] and degradation of weak chain of the matrix [86]. Thermal degradation of natural fibers (*Hibiscus sabdariffa*)-reinforced CSNL composites recorded 10% weight loss at 243.0 °C due to degradation of natural fibers [89]. The final thermal decomposition of composites was at 945.0 °C. The thermal degradation stages indicated that cellulosic material affects the thermal stability of CSNL composites.

The treatment of natural fibers with laccase is well studied as oxido-reductase enzyme. It has a dual character; it causes excessive polymerization or depolymerizes lignin compound through free radical reaction [90, 91]. Thermal stability of laccase-treated and -untreated fibers was observed at two temperatures: first it starts at 300 °C due to amorphous cellulose, and then the crystalline cellulose degrades at higher temperature around 350 °C [92]. It was also found that treated fibers improve the thermal stability. The comparative study of treated and untreated fibers showed that treated fibers increase the thermal stability from 449 to 491 °C. Thermal properties were improved in treated fibers because of their higher crystallinity index (CrI). It was observed that treated fibers improve the thermal stability with increasing the crystallinity of the fiber [20].

Untreated and treated sisal-reinforced composites showed a rapid drop in temperature between 340 and 360 °C, which is mainly due to degradation of materials [93]. The sisal-reinforced PLA composites showed lower thermal stability than pure PLA, which may be due to the thermal degradation of fibers during manufacturing process. The other reason, which maybe alkali treatment, removed the lignin and damaged the cellulosic structure. Lower crystallinity index of treated composites could be another reason as well. In addition, the weight percentage of the residue of three materials differed from the others. Untreated composite had the most residues while the neat PLA had the least. It indicated that

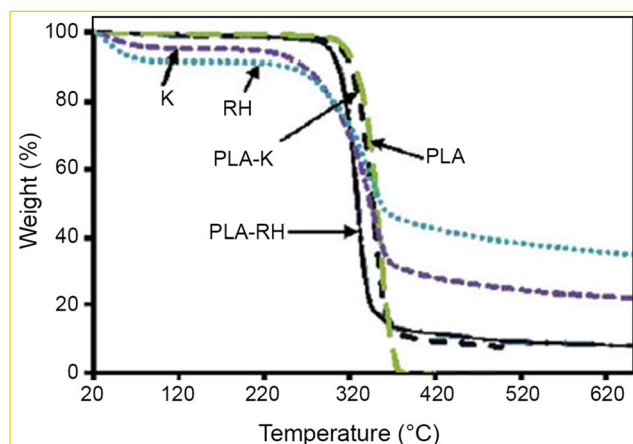


**Fig. 5** Thermogravimetric curves of K, RH, PLA, PLA-K and PLARH [80] (with permission)

sisal fiber/PLA composites had a higher heat resistance than neat PLA because of sisal fibers as reinforcement, and heat resistance of untreated sisal which was better than that of treated sisal [93].

A study on thermal properties of pure PLA and biocomposites with different bamboo char (BC) loadings showed a single-stage decomposition process [94]. Pure PLA revealed higher thermal stability than BC composites because pure PLA required higher temperature to break the molecular chain. By addition of BC to PLA, the molecular mobility was increased and some other molecular chains were decomposed and crystallization was developed due to plasticization and heterogeneous nucleation, which resulted in decreasing of thermal degradation at lower temperature. Another research [95] revealed that starting temperature decreased and then increased, indicating improvement of crystallization and shifting thermal degradation to higher temperatures.

The thermal properties of blended polymer of polyhydroxybutyrate (PHB) and poly(hydroxybutyrate-co-hydroxyvalerate (P(HB-HV)) were investigated by TGA technique and there was no weight loss below 100 °C due to the absence of hydroxyl groups [96]. The thermal degradation of pure PHB showed 5% weight loss at 242 °C; however, the thermal degradation of P(HBHV) was observed at 249 °C. After the addition of natural fibers to PHB and P(HBHV), the thermal stability was improved by 10 °C. Natural fiber-reinforced PHB composites exhibited thermal degradation at 290 °C and natural fiber-reinforced P(HB-HV) composites showed thermal degradation at 270 °C. The higher fiber ratio enhanced the residual amount due to the presence of ashes. A study of Bhardwaj et al. [97] found that addition of cellulose does not produce changes in thermal stability of P(HB-HV), but it can increase the amount of final residue. A study on bleached Kraft soft wood (BKS)W)-reinforced PLA biocomposites by TGA showed the first thermal degradation at 250 °C [98] which was due to the decomposition of hemicelluloses and cellulose [99], shown in Fig. 6. The thermal degradation of pure PLA started from the temperature 300–400 °C. The addition of natural fibers to PLA reduced the thermal stability due to cellulose. The comparative study of kenaf/PLA and rice husk/PLA hybrid composites was performed to compare their thermal behavior [80]. Shibata et al. [100] found that hemicelluloses decompose first, followed by cellulose and lignin. After 360 °C, the weight loss is due to the decomposition of non-cellulosic materials. The thermal degradation of pure PLA was at 323 °C; after the incorporation of kenaf and rice husk the temperature of degradation declined to 321 °C and 305 °C, respectively. Kenaf-reinforced PLA composite showed 75% weight loss at 357 °C, while rice husk/PLA composite degraded at 340 °C. In all conditions, rice husk composite showed less thermal stability than kenaf composite, which may be due to the chemical composition of the two natural fibers [80].

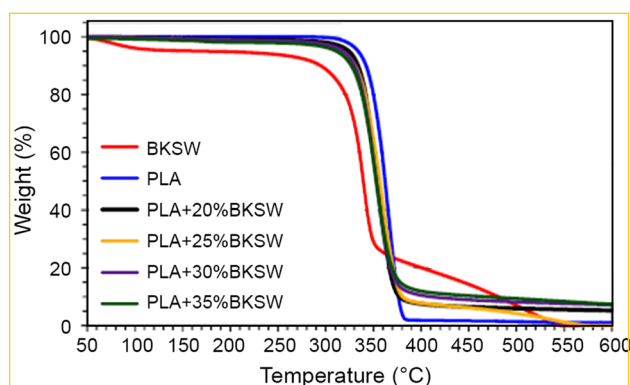


**Fig. 6** TGA of PLA, BKS and PLA composites reinforced with different filler contents [98] (with permission)

## Natural fiber-based hybrid composites

### Hybrid thermoset composites

Many researchers have reported on the thermogravimetric analysis of fiber/filler-reinforced thermoset polymer hybrid composites. Some TGA works are reported based on natural fiber-reinforced thermoset polymer hybrid composites, which are presented in Table 5.

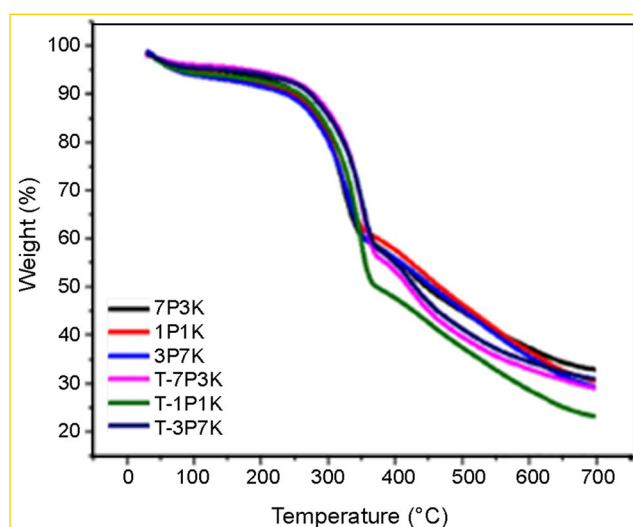
Silane-treated and -untreated PALF/KF-reinforced phenolic hybrid composites presented a major weight loss between 34 and 45% in the temperature range of 278–306 °C, shown in Fig. 7 [101], because of the decomposition of hemicellulose, lignin, pectin and the glycosidic linkages of cellulose [44, 46]. The weight losses of treated hybrid composites were higher, maybe due to partial removal of hemicellulose and lignin. In addition, cellulose was exposed by silane treatment. The silane coating on fibers improved the thermal stability of composites [41]. The DTG curve showed two peaks, which the first peak was below 100 °C due to hydroxyl groups in fibers [49]. The second peaks were due to the degradation of cellulose and hemicellulose of fibers and also the presence of voids and loose fibers presence within composites [101].

The thermal properties of pure epoxy, EFB/epoxy composites and EFB/jute hybrid composites were compared by TGA [102]. EFB/jute hybrid composites improved the thermal stability due to thermal properties of jute fibers. The initial thermal degradations of hybrid composites were between the temperature 270 °C and 300 °C due to breakage of glycosidic linkage of cellulose. The second thermal degradation was due to the degradation of lignin in the temperature range of 340–360 °C [103]. The thermal degradation of hybrid composite started between the temperature range of 250 °C and 400 °C because of decomposition of the cellulosic and hemicellulosic components of the natural fiber in the composites [104]. Hybrid composites started thermal



**Table 5** Thermogravimetric analysis of natural fibers-reinforced hybrid thermoset polymer composites

Reinforcement	Matrix	References
Oil palm empty fruit bunch and woven jute fiber	Epoxy resin	[102]
Banana and flax	Epoxy resin	[195]
Jute fiber and oil palm empty fruit bunch	Epoxy resin	[108]
Kenaf and pineapple leaf fiber	Phenolic resin	[41]
Date palm wood flour/glass fiber	PP	[196]
Kenaf fibers	Poly(vinyl chloride)/thermoplastic polyurethane blend	[124]
Short hemp fiber/glass fiber	PP	[104]
Basalt fiber and hempfiber	High density polyethylene	[8]
Coir and pineapple leaf fiber	Poly(lactic acid)	[137]
Bamboo fiber	Polypropylene/poly(lactic acid) blend	[197]
Natural montmorillonite and organically modified	Potato starch	[198]

**Fig. 7** TGA graph of PALF/kenaf-reinforced thermoset hybrid composites [101] (adopted)

degradation at higher temperature due to presence of jute fibers; it also helps to increase the final residue [102].

TGA of jute/glass/epoxy hybrid composites showed that initial thermal degradation of jute fibers was 31%; however, weight loss of fiber glass was only 1.95%. The final thermal degradation was observed between 200 °C and 450 °C and it degraded approximately 70.70% because of degradation of jute fibers present in epoxy composites. The residual amount of the total mass was recorded by only 6.48%. The TGA curve of thermal degradation of 25% jute fiber and 7% glass fiber hybrid composites showed 1.52% of the weight loss. The final weight loss was recorded between 200 °C and 450 °C, which was approximately 68.97%. Last, the residual amount was only 17.5% of the original mass. Another hybrid composite having different ratio of jute fiber and glass fibers, 18% and 19% respectively, revealed weight loss only 1.27% of the

initial weight. The weight loss in the temperature range of 200–450 °C was approximately 63.54% and the final residual amount was 24.19% of the original mass [105].

Thermogravimetric analysis of pure epoxy, basalt composite and jute/basalt hybrid composite showed that thermal degradation starts around 330 °C with a maximum degradation at 375 °C. Basalt composites started their thermal decomposition at 363 °C, whereas jute/basalt hybrid composite was decomposed in two stages. The first stage of degradation was due to jute fabric decomposition at 250 °C and the second stage was due to epoxy decomposition at 320 °C [106]. The TGA result of jute/banana/epoxy hybrid composites having ratio 1:1 revealed initial temperature of thermal degradation at 200 °C because of the presence of solvent. The highest thermal degradation was found at 380 °C because of the decomposition of matrix and fibers. Jute/banana hybrid composites with fiber ratios of 3:1 and 1:3 revealed major weight loss at 377.72 °C and 376.51 °C, respectively, which is associated with thermal degradation of natural fibers and matrix [107].

In another study on treated and untreated EFB/jute/epoxy hybrid composites, the thermal properties were investigated using TGA curves [108]. The initial weight loss occurred below 100 °C due to water molecules present in the fibers. The major thermal degradation was recorded in the temperature range of 250–450 °C. The initial thermal degradation process of untreated hybrid composites was started in the temperature range of 268–297 °C because of the thermal decomposition of hemicellulose and  $\alpha$ -cellulose [109]. The temperature of final degradation was recorded in the range of 441–462 °C which indicated the complete decomposition of matrix and lignocellulosic materials [110].

The treated hybrid composites revealed the improved thermal stability. The final thermal degradation temperature of treated hybrid composite shifted to higher temperature due to complex reaction with treated chemicals. This behavior of thermal degradability was due to the increase in



the molecular weight resulted from cross-linking reaction between epoxy matrix and lignocellulosic or molecular chain extension of the matrix itself [111, 112].

### Hybrid thermoplastic polymer composites

Thermogravimetric analysis of natural/synthetic fiber/filler-reinforced thermoplastic polymer hybrid composites have been reported by many researchers. Some TGA works on the lignocellulosic material-based thermoplastic hybrid composites are reported in Table 5. TGA of core/shell particle hybrid composites revealed a two-stage thermal degradation process. The alkali-treated hybrid composites showed better thermal stability due to removal of less thermal stable compounds in natural fibers [63, 113]. The hybrid composite curve exhibited stability toward 300 °C. The main thermal degradation of hybrid composites was initiated at higher temperature as compared to pure PP composites [19]. Another study based on thermal stability of bamboo/glass-reinforced PP hybrid composites indicated that higher char residue helps to improve the fire retardancy of materials [114, 115].

TGA analysis of 30% fiber loading of grafted and ungrafted kenaf-reinforced blended poly(vinyl chloride) (PVC)/ethylene vinyl acetate (EVA) composites was investigated [116]. The initial thermal degradations of ungrafted kenaf composites were started in the temperature range of 200–400 °C. The maximum weight loss was recorded by 40% at the temperature 296 °C which was related to the decomposition of hemicellulose and cellulose of fibers. The decomposition of cellulosic materials was due to the dehydration of cellulosic cells and breakage of glycosidic linkage through trans-glycosylation and scission of  $-CO$  and C–C bonds [117]. However, another thermal degradation was found at 480 °C and weight loss was 84.1%. The addition of ungrafted kenaf fibers to the PVC/EVA blend matrix did not affect the degradation behavior. However, the grafted kenaf composites revealed that the initial thermal degradation occurred at 276 °C corresponding to the hemicellulose and lignin decomposition, and the second decomposition was at 290 °C due to lignin decomposition. The final thermal degradation was observed at 414 °C, resulted from degradation of poly(methyl methacrylate) (PMMA). The DTG curves revealed that grafting of kenaf fibers reduced the thermal properties compared to ungrafted kenaf composite.

Another study based on the thermal degradations of sugar palm/glass fibers/thermoplastic polyurethane hybrid composites was done by TGA, whose results are shown in Fig. 8 [118]. All types of hybrid composites revealed three steps of weight loss. Clearly, the first thermal degradation was due to the natural fibers' degradation and then decomposition of glass fibers and last, the weight loss due to thermoplastic

polyurethane (TPU). The higher ratio of sugar palm fibers and lower glass fibers increased the thermal degradation at lower temperature. The thermal degradation of pure glass fiber composite showed a weight loss of about 39.6% between 200 and 450 °C, which is related to decomposition of the main constituent of sugar palm fibers. The residual amount was 60.4% of initial mass. The DTG curve revealed a small peak between 230 and 330 °C corresponding to the thermal degradation of organic elements, while the second peaks were due to hemicellulose degradation in the range of 340–390 °C. The third weight loss at 400 °C and 480 °C was due to degradation of cellulose of fiber. A higher ratio of glass fibers led to thermal degradation at higher temperature of 435 °C. Addition of sugar palm increased the weight loss, but the maximum temperature of thermal decomposition was the same as that of pure glass fiber composite that was the indication of the improvement in thermal stability of sugar palm fibers with TPU composites. The similar result of thermal degradation was also reported for jute–glass fiber composites [105].

Another study [119] based on the thermal stability of sisal fiber/glass fiber/PP hybrid composites revealed thermal degradation at higher temperature. The thermal stability which was due to the molecular weight and caused by good compatibility of matrix and reinforced materials and the extension of molecular chain of PP by the compatibilizers [116]. Due to the addition of compatibilizer, the hybrid composites showed an insignificant thermal degradation at 200 °C compared to the pure sisal composites. A work reported on sisal fibers showed that the thermal degradation of sisal fibers was 8% at 200 °C due to the decomposition of hemicellulose [120]. Further improvement in thermal stability of

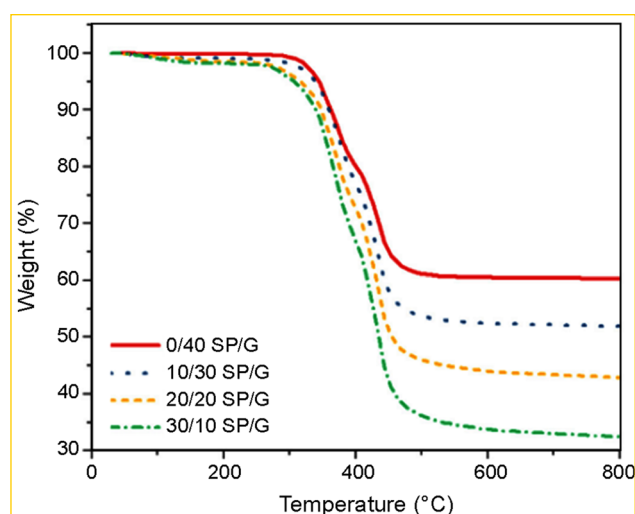


**Fig. 8** TGA analysis of SP/G-reinforced TPU hybrid composites [118] (with permission)

sisal composite, using thermal stabilizer in polymer or pretreatment of fibre is recommended [121, 122].

Thermal property of sisal/glass fiber/PP hybrid biocomposite was studied using TGA [123]. The result showed the addition of glass fibers improved the thermal stability. The peak at 190–375.8 °C was due to the degradation of cellulose and hemicellulose, while the second peak was observed between 190 and 230 °C for various fiber loadings of hybrid composites. Compared to pure sisal composite, the temperature of thermal degradation at the third peak of the sisal/glass hybrid composite was increased from 340 to 380 °C.

Thermal degradation of poly(vinyl chloride) (PVC)/thermoplastic polyurethane (TPU)/kenaf fiber hybrid composite at various fiber loadings revealed an initial mass loss in the temperature range of 25–188 °C due to hydroxyl groups [124]. The second weight loss was at temperature 188–500 °C. The PVC/TPU/KF composites revealed high thermal degradation due to decomposition of hemicelluloses [26]. The composites having higher natural fiber content showed higher weight loss in the range of 250–300 °C. It showed that lower natural fiber in the composites had better thermal properties. The last DTG curve of mass loss showed that the introduction of kenaf into the PVC/TPU increased the maximum degradation peak from 275 to 281.7 °C due to the kenaf properties.

The thermal degradation curve of seaweed (Sw)/SPF hybrid composite revealed multiple steps of degradation [125]. The initial weight loss below 100 °C was due to the high moisture content and lower molecular weight compound [126]. The second weight loss which was recorded between 100 and 200 °C was associated with the hydroxyl group and glycerol [127]. The thermal degradation of agar was recorded above the temperature of 270 °C [128]. The maximum thermal degradation of starch carbon chain was found at temperature of 300 °C [129]; however, carbohydrate and protein from seaweed were recorded in the range of 180–450 °C [130]. The thermal degradation range from 200 to 270 °C showed the decomposition of hemicellulose and cellulose; however, lignin degraded at higher temperature range of 270–370 °C. The final thermal degradation beyond the temperature 500 °C showed carbonate degradation in seaweed that could help to form char [131].

A study on rice husks and sawdust used as filler in filled recycled high-density polyethylene (rHDPE) was done by thermogravimetric analysis to investigate thermo-oxidative degradation behavior under atmospheric air flow condition [132]. Addition of antioxidants (AOs) was not effective to control degradation mechanism of composites. Various ratios of AOs also showed almost the same trend; nevertheless the final residue for composites having 0.5% AOs was higher. Comparative study of without/with fire retardant (FRs) revealed the composite with FRs had improved thermal stability. Composites with FRs started to decompose

near 300 °C due to lower thermal stability of saw dust than the rice husks and matrix. The thermal degradation of rice husk started above the temperature 350 °C; however, the rHDPE degraded slowly until the temperature reached 500 °C. The properties of the fire retardant develop a barrier by effective silica layer formed during the combustion process or thermal shielding by adding flame retardant agents that slow the burning reaction. The silica content in the rice husk plays a specific synergistic role as fire retardant/thermal resistant for the materials [133, 134].

## Hybrid biopolymer composites

Hybridization of different types of synthetic and natural fibers in polymer composite has been widely accepted for better thermal and mechanical properties of composite materials and also for overcoming the drawbacks of natural fiber [135]. Solely, reinforcement of natural fibers is not very encouraged in polymer composites, but environmentally it shows the positive potential in structural purposes. The studies are conducted on the hybridization of different types of natural fibers into polymer composites to improve the mechanical, physical and thermal properties [52, 136], as shown in Table 5.

Thermal properties of PALF/coir-reinforced PLA hybrid composites were investigated at various fibers ratios, as seen in Fig. 9 [137]. Thermal properties of pure PLA and hybrid composites revealed a two-step degradation process. The first step showed the degradation of hemicellulose of composites and hybrid composites in the range of 200–300 °C. Another range between 400 and 500 °C was related to the decomposition of lignin and cellulose [26]. The lower  $T_g$  and the least final residue were observed for PLA; however, the hybrid composites with 1:1 ratio of coir/PALF and 7:3 ratio of coir/PALF showed higher  $T_g$  values of 290.07 °C and 288.64 °C, respectively. The differences in thermal

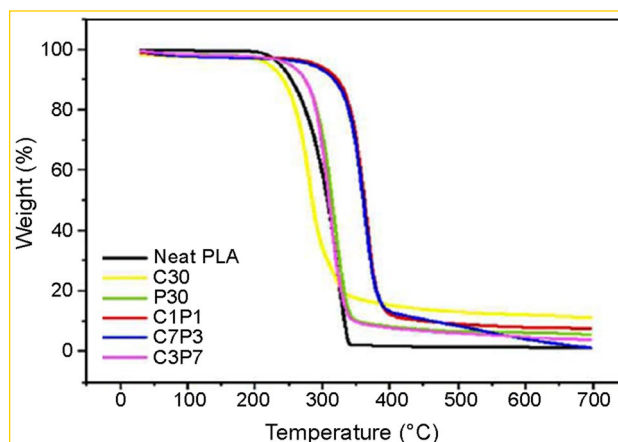


Fig. 9 TGA of PALF/coir-reinforced PLA hybrid composites [137]

properties are due to the primary constituents of natural fibers such as PALF which has low lignin [13] and coir which has high percentage of lignin [138]. Further, PALF/coir-reinforced PLA hybrid composites have been studied after surface modification of fibers and comparing the properties [139]. Thermal stability of EFB/kenaf/PLA hybrid composite was studied by TGA that showed the weight loss for all composites at the temperature range of 55–135 °C due to hydroxy groups [140]. The thermal degradation of kenaf/PLA composite was observed around 270 °C; however, the EFB/PLA and EFB/kenaf/PLA revealed the same temperature of 240 °C for thermal degradation. Kenaf showed better interaction and homogeneous distribution than EFB with PLA and it showed insignificant thermal properties of EFB/kenaf/PLA hybrid composites.

The thermograms of pure PLA, benzoyl peroxide-treated and untreated banana/sisal fiber hybrid composites exhibit a single-stage weight loss [141]. The thermal degradation temperature of pure PLA (334 °C) was lower than that of untreated hybrid composites (342 °C) and treated hybrid composites (349 °C). The final residual amount of PLA was very low (0.23%) which showed the least thermal stability compared to hybrid composites. The thermal degradation of PLA was due to chain scission, formation of lactide monomers and cleavage of ester bonds that occurred at higher temperatures [142]. The untreated hybrid composites began thermal decomposition from 342 to 373 °C and the delayed thermal degradation exhibited that natural fibers in PLA led to a better thermo-oxidative stability due to presence of lignin in fibers [13, 143]. The final thermal degradations occurred at 373 °C due to presence of D-xylose and L-arabinose in the fibers. The aromatic reaction due to the presence of lignin and further dehydration reaction were main causes of breaking the chemical chain of proto-lignin available in the untreated banana and sisal fiber [144]. The initial degradation of treated hybrid composites showed maximum peak at 378.8 °C corresponding to a 90% weight loss. Benzoyl peroxide is known for its effect on the cellulose structure leading to better thermal stability. The treatments of natural fibers partly wash out the hemicellulose and lignin and further react with the hydroxyl groups of cellulose and polymers [13, 145]. Final degradation of hybrid composites revealed the cellulose decomposition through cleavage of glycoside bonds such as CAH, CAO, CAC bonds and other processes like dehydration, decarboxylation and decarbonylation [146]. Surface treatment of hybrid composites showed strong cross-linking reaction between the matrix and fibers and restricted the molecular movement which improved thermal stability [143]. The thermal properties of pure cashew gum (CG), gelatin (G) and the CG/G hybrid films were investigated [147]. CG and CG/G revealed weight loss in three stages; however, gelatin showed only two steps of thermal degradation. The initial stage thermal

decomposition in CG and CG/G was due to water molecules. The second stage of thermal degradation of CG and CG/G film was observed near the temperature of 264 °C and 257 °C, respectively, because of having low molecular weight proteins and polysaccharide components and glycerol evaporation [148]. The third weight loss temperature at 331 °C for CG, at 341 °C for G and at 323 °C for CG/G films revealed the decomposition of the gelatin backbone and the cashew gum, and the same type of research was reported about carboxymethyl cellulose-cassava starch films [149], gelatin/chitosan films [150] and cassava starch-based films [151]. Among all films, CG/G film showed the highest residual amount (22%) and pure gelatin and cashew gum had 19% and 14% residual amount, respectively. Gelatin has been shown to help the thermal stability of CG/G film.

Thermal degradation behavior of untreated, keratin biofiber treated with polyhedral oligomeric silsesquioxanes (POSS) and nanoclay/biofiber composites was investigated [152]. Unmodified and modified clay fiber showed weight loss below 200 °C that was attributed to the presence of hydroxyl group which may be due to air trap during the mixing process of nanoclay. In case of treated fiber with POSS, weight loss was absent below 200 °C that indicated the treated fibers are more hydrophilic in nature due to grafting of POSS molecules on the surface of the fiber which reduces number of polar groups. The first stage of decomposition of neat fiber and POSS modified fibers were 205 °C and 227 °C, respectively. Grafting of POSS nanocages improved thermo-oxidative stability which delayed maximum weight loss compared to pure keratin fiber. In another research, it is found that weight loss temperature increased from 441 °C to 573 °C due to increment in char yield which resist oxidation process and improve the flame retardancy of the materials [151].

## Hybrid nanocomposites

In fabrication and processing, the nanocomposites are very similar to the conventional polymer composites and the easier way of fabrication makes the nanocomposite more attractive [153]. Nanocomposites are more prominent of the conventional composites due to their light weight, good dimensional stability, enhanced heat and flame resistance, as well as barrier properties with far less loading of nanoparticles [154].

DTG curves of silver nanoparticles filler PLA composites showed that addition of silver nanoparticles up to 1% influenced the thermal stability insignificantly. The thermal degradation temperature of 5% microcrystalline cellulose (5MCC)/PLA shifted to lower temperature, and further addition of 1% of Ag decreased the temperature of thermal degradation about 25 °C [90]. TGA properties of all pine wood flour/zeolite hybrid composites were moderately stable up

to the temperature above 200 °C, which is higher than the process temperatures for the twin-screw extruder and injection molding. The first thermal decomposition was around 230 °C and the second peaks were around 420 °C. The final residue of zeolite-containing composite was lower than that of wood flour composite [155].

Thermal properties of kenaf/graphene nanoplates/PP/MAPP nanocomposites revealed the effect of graphene nanoplates (GNP) on thermal stability of PP composite [156]. GNP loading of 3 phr showed the highest thermal stability due to high GNP aspect ratio and uniform distribution which provided barrier protection and hindered evolution of gaseous molecules during thermal decomposition. Uniformly dispersed GNP hindered the supply of oxygen through formation of layers of char on nanocomposites' surface thereby improving thermal stability. The composites exhibited single-step degradation peak in the range of 473–490 °C. The temperature of thermal degradation and char content increased with increasing inclusion of GNP.

Researchers investigated the untreated and treated bamboo/PLA composites and compared them with nanoclay/bamboo/PLA hybrid composites [157]. Initial and final thermal degradation temperatures of untreated bamboo composites were 284 °C and 372 °C, respectively. TGA curve of treated bamboo composites revealed marginally higher initial and final thermal degradation temperatures of 286 °C and 3738 °C due to silane treatment on fiber [158]. During the surface modification of fibers, the ethoxy groups in APS are hydrolyzed to reactive silanol in the presence of water–ethanol mixture. One end of the silanol forms hydrogen bond with free hydroxyl group of fiber and another end reacts with the hydroxyl group of PLA. Addition of nanoclay (3 wt%) remarkably improved the thermal properties of bionanocomposites. Nanoclay/treated bamboo/PLA nanocomposite showed initial and final decomposition temperatures at 295 °C and 385 °C, respectively, and residual amount was 9.55%. Nanoclay was dispersed homogeneously and acted as a gas barrier in form of a volatile by-product [159].

Thermal properties of untreated and treated bamboo cellulose nanowhiskers (BCNW)/PLA composites changed from 100 to 150 °C due to dehydration of water molecules, as shown in Fig. 10 [160]. 1 wt% and 16 wt% treatment of silane showed lower thermal stability than untreated samples; however, 4 wt% treatment of composites improved the thermal stability. The untreated composites revealed high heat transfer within composites due to poor compatibility of PLA and untreated BCNW [161], which makes the thermal stability relatively higher compared to treated composites. Silane treatment with 4 wt% improved the interfacial property that connects with molecular chains of PLA tightly which requires high energy to break down into chemical and physical interactions [162]. Excess amount of silane started

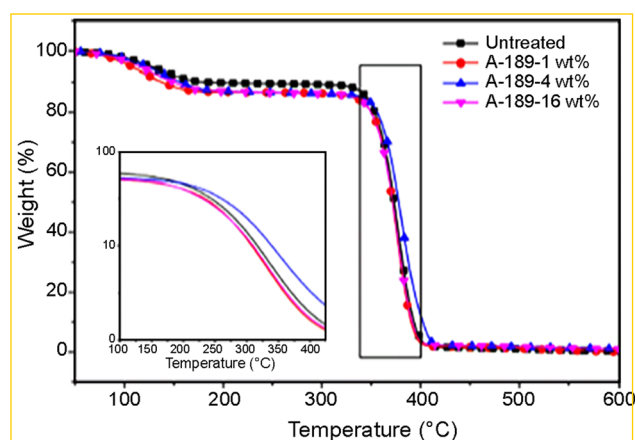


**Fig. 10** TGA of untreated and treated bamboo cellulose nanowhiskers (BCNW)/PLA composites [160] (with permission)

self-condensation reaction with BCNW and PLA molecule [163] and reduced thermal stability.

The thermal stability of chitosan (CS)/bionanocomposite films and various oxidized nanocelluloses (ONC) and polymorphisms (CI and CII) was investigated [164]. Initial thermal degradation was located near 100 °C due to acetic acid and hydroxyl groups [165]. The higher thermal degradation of bionanocomposite films was found in the range of 200–400 °C due to the degradation of CS and ONC. It can be seen that initial thermal decomposition and maximum peak of the blend improved slightly due to ONC polymorphs but the maximum peaks were laid between those of neat CS and the ONC. The comparative study of untreated and benzylated wheat straw nanocomposites was done based on the thermal properties [166]. The thermal decomposition of untreated composites occurred in two steps. The first thermal decomposition step showed 66.37% weight loss in the temperature range of 230 °C and 380 °C due to hydroxyl groups and degradation of hemicellulose and cellulose of fibers. The second weight loss was about 24.45% attributed to degradation of lignin between the temperature range of 380 and 500 °C which showed higher thermal stability than that of hemicellulose and cellulose. After 500 °C there was no weight loss recorded, what means  $\text{Al}_2\text{O}_3$  and  $\text{SiO}_2$  were present in residue and stable at higher temperatures [167]. Benzylated wheat straw nanocomposites showed thermal degradation at higher temperature. After adding nanoclay (5 wt%) thermal properties improved the mechanism of nanoclay in composites, a protective barrier of ablative silicate layers on the remaining polymer [168] is formed by torturous path for volatile products whereby volatilization might be delayed [169]. The silicate layers in each BWS matrix are dispersed in any way and act as a barrier to heat transfer and thermal insulation, reducing the thermal degradation of the specimens to temperatures of 400 °C.



Thermal stability of cellulose nanocrystals (CNC)/graphene (GR)/PLA nanocomposites showed a significant mass loss (> 94 wt%) between 280 and 380 °C due to polymer backbone degradation [170]. The film, which contains 50/50 CNC and GR nanofillers, showed the highest thermal stability, which showed that the combination of these two nanofillers has the highest thermal properties of the film.  $T_g$  values of PLA nanocomposites slightly increased compared to that of the PLA, attributed to the chain mobility restriction produced by the addition of nanofillers. In the case of CNC50/GR50, the cold crystallization temperature (TCC) was shifted towards a higher temperature. In this case, the presence of both nanofillers in the same ratio resulted in a slower crystallization that may be attributed to a more heterogeneous crystallization process. The PLA-T showed a degree of crystallinity of 24.4% which increased in all the PLA nanocomposites. Remarkably, the crystallinity degree was raised up to 31.1% in the case of PLA-CNC95/5GR and 34.6% for the PLA-GR system. The effect of plasticizers and nucleating agents has been already reported, and a broadening of the crystallization temperature window and the crystallization rate is expected from the combination of them [171]. Nucleating agents provide a heterogeneous nucleation at elevated temperatures when the driving force for homogeneous nucleation is weak, while plasticizer improves the crystallization at lower temperatures and allowing the chain mobility.

## Conclusion

The thermal behavior of natural fibers apparently bears a correlation with their chemical constituents such as cellulose, hemicellulose and lignin. Initial weight loss in natural fibers between the temperature 50 and 100 °C is associated with the evaporation of hydroxyl groups from the fiber surface. Isothermal and non-isothermal thermogravimetric analysis showed how the pyrolysis process works in both conditions, and also by using TGA process, LOI can be calculated. Thermal degradation of lignin and cellulose was recorded between 300 and 450 °C, while hemicelluloses being an amorphous material degraded in the temperature range of 200–300 °C. Approximately 60% of the thermal decomposition of most natural fibers occurred within a temperature range between 230 and 350 °C. Beyond temperature 450 °C, the residue could be assigned as char or other products from decomposition reactions. Surface modified natural fibers revealed less mass loss in initial stage, indicating that the treatment partially makes the fibers somewhat hydrophilic in nature.

The initial weight loss is due to the evaporation of moisture from the fiber surface, since the polymeric matrix contribution, if any, should be relatively small. For practical

use, however, the temperature related to the onset of thermal degradation can be considered as the composite thermal stability limit [172]. The natural fiber-reinforced composites revealed weight loss below 100 °C and showed that moisture was absorbed during the manufacturing process of composite. At high temperature, natural fiber-reinforced composites showed better thermal stability than natural fibers alone. The treated fibers further improved the thermal properties due to better interfacial bonding between fibers and matrix. Better fiber–matrix bond covers the fibers thoroughly and protects the fibers by avoiding direct contact with temperature, but treated fiber-reinforced composites mostly showed lower residual amount due to the partially wash out of lignin during treatment process. Thermal degradation is more dependent on the nature of polymers; therefore, thermosets are highly more stable than thermoplastics. The thermal degradation of hybrid composites was affected by different type of fibers due to variety in chemical constituents. The nanocomposites showed better thermal stability due to nano-size filler which acts as thermal resistant materials.

The improvement of thermal stability in natural fiber-reinforced polymer composites has great concern in advanced materials. There are many works that are reported above in various circumstances which can help in selections of materials for a specific purpose. Still, the natural fiber-reinforced polymer composites are being investigated to advance their thermal resistant properties by using nanoparticles, fire retardants and naturally thermal resistant lignocellulosic fibers.

**Acknowledgements** The authors would like to express their gratitude and sincere appreciation to the Department of Biocomposite and Technology, and Institute of Tropical Forestry and Forest Products (INTROP), Universiti Putra Malaysia for their scientific assistance and support to help accomplish this study.

## References

1. Asim M, Jawaid M, Abdan K, Ishak M (2018) The effect of silane treated fiber loading on mechanical properties of pineapple leaf/kenaf fiber filler phenolic composites. *J Polym Environ* 26:1520–1527
2. Cordeiro EP, Pita VJ, Soares BG (2017) Epoxy-fiber of peach palm trees composites: the effect of composition and fiber modification on mechanical and dynamic mechanical properties. *J Polym Environ* 25:913–924
3. Saba N, Jawaid M, Allothman OY, Paridah M, Hassan A (2016) Recent advances in epoxy resin, natural fiber-reinforced epoxy composites and their applications. *J Reinf Plast Compos* 35:447–470
4. Asim M, Jawaid M, Abdan K, Ishak M (2017) Dimensional stability of pineapple leaf fiber reinforced phenolic composites. In: AIP conference proceedings, vol 1901, pp 030016
5. Nasir M, Khali D, Jawaid M, Tahir P, Siakeng R, Asim M, Khan T (2019) Recent development in binderless fiber-board



- fabrication from agricultural residues: a review. *Const Build Mater* 211:502–516
6. Lau KT, Hung PY, Zhu MH, Hui D (2018) Properties of natural fiber composites for structural engineering applications. *Compos B* 136:222–233
  7. Agrebi F, Hammami H, Asim M, Jawaid M, Kallel A (2020) Impact of silane treatment on the dielectric properties of pineapple leaf/kenaf fiber reinforced phenolic composites. *J Compos Mater* 54:937–946
  8. Sarasini F, Tirillò J, Sergi C, Seghini MC, Cozzarini L, Graupner N (2018) Effect of basalt fiber hybridisation and sizing removal on mechanical and thermal properties of hemp fiber reinforced HDPE composites. *Compos Struct* 188:394–406
  9. Siakeng R, Jawaid M, Ariffin H, Sapuan S, Asim M, Saba N (2019) Natural fiber reinforced polylactic acid composites: a review. *Polym Compos* 40:446–463
  10. Akampumuza O, Wambua P, Ahmed A, Li W, Qin XH (2017) Review of the applications of biocomposites in the automotive industry. *Polym Compos* 38:2553–2569
  11. Asim M, Jawaid M, Saba N, Nasir M, Sultan MTH (2017) Processing of hybrid polymer composites—a review. In: *Hybrid polymer composite materials*, vol 2. Elsevier, pp 1–22
  12. Global natural fiber composite market 2015–2020: trends, forecast, and opportunity analysis, December 2015
  13. Monteiro SN, Calado V, Rodriguez RJS, Margem FM (2012) Thermogravimetric behavior of natural fibers reinforced polymer composites: an overview. *Mater Sci Eng A* 557:17–28
  14. Asim M, Jawaid M, Abdan K, Nasir M (2018) Effect of alkali treatments on physical and mechanical strength of pineapple leaf fibers. *IOP Conf Ser: Mater Sci Eng* 290:012030
  15. Methacanon P, Weerawatsophon U, Sumransin N, Prahsarn C, Bergado D (2010) Properties and potential application of the selected natural fibers as limited life geotextiles. *Carbohydr Polym* 82:1090–1096
  16. Yao F, Wu Q, Lei Y, Guo W, Xu Y (2008) Thermal decomposition kinetics of natural fibers: activation energy with dynamic thermogravimetric analysis. *Polym Degrad Stab* 93:90–98
  17. Beg MDH, Pickering KL (2008) Accelerated weathering of unbleached and bleached Kraft wood fiber reinforced polypropylene composites. *Polym Degrad Stab* 93:1939–1946
  18. Puglia D, Monti M, Santulli C, Sarasini F, De Rosa IM, Kenny JM (2013) Effect of alkali and silane treatments on mechanical and thermal behavior of *Phormium tenax* fibers. *Fiber Polym* 14:423–427
  19. Essabir H, Bensalah M, Rodrigue D, Bouhfid R, Quais A (2016) Structural, mechanical and thermal properties of bio-based hybrid composites from waste coir residues: fibers and shell particles. *Mech Mater* 93:134–144
  20. Nasir M, Sulaiman O, Hashim R, Hossain K, Gupta A, Asim M (2015) Rubberwood fiber treatment by laccase enzyme and its application in medium density fiberboard. *J Pure Appl Microbiol* 9:2095–2100
  21. Ray D, Sarkar BK, Rana A, Bose NR (2001) The mechanical properties of vinyl ester resin matrix composites reinforced with alkali-treated jute fibers. *Compos A* 32:119–127
  22. Alvarez V, Rodriguez E, Vázquez A (2006) Thermal degradation and decomposition of jute/vinylester composites. *J Therm Anal Calorim* 85:383–389
  23. Alabdulkarem A, Ali M, Iannace G, Sadek S, Almuzaiqer R (2018) Thermal analysis, microstructure and acoustic characteristics of some hybrid natural insulating materials. *Constr Build Mater* 187:185–196
  24. Abu-Sharkh B, Hamid H (2004) Degradation study of date palm fiber/polypropylene composites in natural and artificial weathering: mechanical and thermal analysis. *Polym Degrad Stab* 85:967–973
  25. Wang W, Sain M, Cooper P (2005) Hygrothermal weathering of rice hull/HDPE composites under extreme climatic conditions. *Polym Degrad Stab* 90:540–545
  26. Azwa Z, Yousif B, Manalo A, Karunasena W (2013) A review on the degradability of polymeric composites based on natural fibers. *Mater Des* 47:424–442
  27. Głowińska E, Datta J, Parcheta P (2017) Effect of sisal fiber filler on thermal properties of bio-based polyurethane composites. *J Therm Anal Calorim* 130:113–122
  28. Alvarez V, Vázquez A (2004) Thermal degradation of cellulose derivatives/starch blends and sisal fiber biocomposites. *Polym Degrad Stab* 84:13–21
  29. Chen WH, Kuo PC (2011) Isothermal torrefaction kinetics of hemicellulose, cellulose, lignin and xylan using thermogravimetric analysis. *Energy* 36:6451–6460
  30. Hillier J, Bezzant T, Fletcher TH (2010) Improved method for the determination of kinetic parameters from non-isothermal thermogravimetric analysis (TGA) data. *Energy Fuel* 24:2841–2847
  31. Dhyani V, Bhaskar T (2018) Kinetic analysis of biomass pyrolysis. *Waste Biorefin* 2018:39–83
  32. Sharma P, Choudhary V, Narula AK (2008) Effect of structure of aromatic imide-amines on curing behavior and thermal stability of diglycidyl ether of bisphenol-A. *J Appl Polym Sci* 107:1946–1953
  33. Ferdosian F, Yuan Z, Anderson M, Xu CC (2016) Thermal performance and thermal decomposition kinetics of lignin-based epoxy resins. *J Anal Appl Pyrol* 119:124–132
  34. Nelson M (2001) A dynamical systems model of the limiting oxygen index test: II. retardancy due to char formation and addition of inert fillers. *Combust Theor Model* 5:59–83
  35. Basnet S, Otsuka M, Sasaki C, Asada C, Nakamura Y (2015) Functionalization of the active ingredients of Japanese green tea (*Camellia sinensis*) for the synthesis of bio-based epoxy resin. *Ind Crops Prod* 73:63–72
  36. Aouf C, Le Guernevé C, Caillol S, Fulcrand H (2013) Study of the *O*-glycidylation of natural phenolic compounds: the relationship between the phenolic structure and the reaction mechanism. *Tetrahedron* 69:1345–1353
  37. Benyahya S, Aouf C, Caillol S, Boutevin B, Pascault JP, Fulcrand H (2014) Functionalized green tea tannins as phenolic prepolymers for bio-based epoxy resins. *Ind Crops Prod* 53:296–307
  38. Ross CF, Hoyer C Jr, Fernandez-Plotka VC (2011) Influence of heating on the polyphenolic content and antioxidant activity of grape seed flour. *J Food Sci* 76:C884–C890
  39. Khalil HA, Marliana MM, Alshammari T (2011) Material properties of epoxy-reinforced biocomposites with lignin from empty fruit bunch as curing agent. *BioResources* 6:5206–5223
  40. Aji IS, Zainudin ES, Khalina A, Sapuan SM, Khairul MD (2012) Thermal property determination of hybridized kenaf/PALF reinforced HDPE composite by thermogravimetric analysis. *J Therm Anal Calorim* 109:893–900
  41. Asim M, Jawaid M, Paridah MT, Saba N, Nasir M, Shahroze RM (2019) Dynamic and thermo-mechanical properties of hybridized kenaf/PALF reinforced phenolic composites. *Polym Compos* 40:3814–3822
  42. De Rosa IM, Santulli C, Sarasini F (2010) Mechanical and thermal characterization of epoxy composites reinforced with random and quasi-unidirectional untreated *Phormium tenax* leaf fibers. *Mater Des* 31:2397–2405
  43. Manfredi LB, Rodríguez ES, Władysław-Przybylak M, Vázquez A (2006) Thermal degradation and fire resistance of unsaturated polyester, modified acrylic resins and their composites with natural fibers. *Polym Degrad Stab* 91:255–261
  44. Arbelaz A, Fernandez B, Ramos J, Mondragon I (2006) Thermal and crystallization studies of short flax fiber reinforced

- polypropylene matrix composites: effect of treatments. *Thermochim Acta* 440:111–121
45. Yang H, Yan R, Chen H, Lee DH, Zheng C (2007) Characteristics of hemicellulose, cellulose and lignin pyrolysis. *Fuel* 86:1781–1788
  46. Kumar SS, Duraibabu D, Subramanian K (2014) Studies on mechanical, thermal and dynamic mechanical properties of untreated (raw) and treated coconut sheath fiber reinforced epoxy composites. *Mater Des* 59:63–69
  47. Biswas S, Shahinur S, Hasan M, Ahsan Q (2015) Physical, mechanical and thermal properties of jute and bamboo fiber reinforced unidirectional epoxy composites. *Procedia Eng* 105:933–939
  48. Gheith MH, Aziz MA, Ghorri W, Saba N, Asim M, Jawaid M, Alothman OY (2019) Flexural, thermal and dynamic mechanical properties of date palm fibers reinforced epoxy composites. *J Mater Res Technol* 8:853–860
  49. Ridzuan M, Majid MA, Afendi M, Mazlee M, Gibson A (2016) Thermal behaviour and dynamic mechanical analysis of *Penisetum purpureum*/glass-reinforced epoxy hybrid composites. *Compos Struct* 152:850–859
  50. Asim M, Jawaid M, Abdan K, Ishak MR (2016) Effect of alkali and silane treatments on mechanical and fiber-matrix bond strength of kenaf and pineapple leaf fibers. *J Bionic Eng* 13:426–435
  51. Zadeh KM, Ponnammma D, Al-Maadeed MAA (2017) Date palm fiber filled recycled ternary polymer blend composites with enhanced flame retardancy. *Polym Test* 61:341–348
  52. Asim M, Jawaid M, Nasir M, Saba N (2018) Effect of fiber loadings and treatment on dynamic mechanical, thermal and flammability properties of pineapple leaf fiber and kenaf phenolic composites. *J Renew Mater* 6:383–393
  53. Nair KM, Thomas S, Groeninckx G (2001) Thermal and dynamic mechanical analysis of polystyrene composites reinforced with short sisal fibers. *Compos Sci Technol* 61:2519–2529
  54. Lee YK, Kim DI, Kim HJ, Hwang TS, Rafailovich M, Sokolov J (2003) Activation energy and curing behavior of resol- and novolac-type phenolic resins by differential scanning calorimetry and thermogravimetric analysis. *J Appl Polym Sci* 89:2589–2596
  55. Sreekala M, Kumaran M, Thomas S (1997) Oil palm fibers: morphology, chemical composition, surface modification, and mechanical properties. *J Appl Polym Sci* 66:821–835
  56. Akter M, Jahan E, Hasan M (2018) Mechanical, thermal and morphological properties of pineapple and betel nut husk fiber reinforced hybrid polypropylene composites. In: *IOP Conference Series: Mater Sci Eng*, 2018, vol 1. IOP Publishing, pp 012026
  57. Santos EF, Mauler RS, Nachtigall SM (2009) Effectiveness of maleated and silanized-PP for coir fiber-filled composites. *J Reinf Plast Compos* 28:2119–2129
  58. El-Sabbagh A (2014) Effect of coupling agent on natural fiber in natural fiber/polypropylene composites on mechanical and thermal behaviour. *Compos B* 57:126–135
  59. El-Shekeil Y, Sapuan S, Abdan K, Zainudin E (2012) Influence of fiber content on the mechanical and thermal properties of Kenaf fiber reinforced thermoplastic polyurethane composites. *Mater Des* 40:299–303
  60. Beyler CL, Hirschler MM (2002) Thermal decomposition of polymers. *SFPE Handb Fire Protect Eng* 2:111–131
  61. Beckermann G, Pickering KL (2008) Engineering and evaluation of hemp fiber reinforced polypropylene composites: fiber treatment and matrix modification. *Compos A* 39:979–988
  62. Arrakhiz F, El Achaby M, Maïha M, Bensalah M, Fassi-Fehri O, Bouhfid R, Benmoussa K, Qaiss A (2013) Mechanical and thermal properties of natural fibers reinforced polymer composites: Doum/low density polyethylene. *Mater Des* 43:200–205
  63. Arrakhiz F, El Achaby M, Benmoussa K, Bouhfid R, Essassi E, Qaiss A (2012) Evaluation of mechanical and thermal properties of Pine cone fibers reinforced compatibilized polypropylene. *Mater Des* 40:528–535
  64. Pracella M, Haque MM-U, Alvarez V (2010) Functionalization, compatibilization and properties of polyolefin composites with natural fibers. *Polymer* 51:554–574
  65. Araujo J, Waldman W, De Paoli M (2008) Thermal properties of high density polyethylene composites with natural fibers: coupling agent effect. *Polym Degrad Stab* 93:1770–1775
  66. Mohanty S, Verma SK, Nayak SK (2006) Dynamic mechanical and thermal properties of MAPE treated jute/HDPE composites. *Compos Sci Technol* 66:538–547
  67. Rana A, Mandal A, Bandyopadhyay S (2003) Short jute fiber reinforced polypropylene composites: effect of compatibiliser, impact modifier and fiber loading. *Compos Sci Technol* 63:801–806
  68. Halden RU (2010) Plastics and health risks. *Annu Rev Publ Health* 31:179–194
  69. Williams CK, Hillmyer MA (2008) Polymers from renewable resources: a perspective for a special issue of polymer reviews. *Polym Rev* 48:1–10
  70. Fertier L, Koleilat H, Stemmelen M, Giani O, Joly-Duhamel C, Lapinte V, Robin JJ (2013) The use of renewable feedstock in UV-curable materials—a new age for polymers and green chemistry. *Prog Polym Sci* 38:932–962
  71. Laurichesse S, Avérous L (2014) Chemical modification of lignins: towards biobased polymers. *Prog Polym Sci* 39:1266–1290
  72. USDA N (2015) Crop Production 2014 Summary. National Agricultural Statistics Service United States, Department of Agriculture, Washington
  73. Zhang C, Garrison TF, Madbouly SA, Kessler MR (2017) Recent advances in vegetable oil-based polymers and their composites. *Prog Polym Sci* 71:91–143
  74. Goriparthi BK, Suman K, Rao NM (2012) Effect of fiber surface treatments on mechanical and abrasive wear performance of polylactide/jute composites. *Compos A* 43:1800–1808
  75. Kabir M, Wang H, Lau K, Cardona F, Aravinthan T (2012) Mechanical properties of chemically-treated hemp fiber reinforced sandwich composites. *Compos B* 43:159–169
  76. Rosa MF, Chiou B-s, Medeiros ES, Wood DF, Williams TG, Mattoso LH, Orts WJ, Imam SH (2009) Effect of fiber treatments on tensile and thermal properties of starch/ethylene vinyl alcohol copolymers/coir biocomposites. *Bioresour Technol* 100:5196–5202
  77. Bakare I, Okieimen F, Pavithran C, Khalil HA, Brahmakumar M (2010) Mechanical and thermal properties of sisal fiber-reinforced rubber seed oil-based polyurethane composites. *Mater Des* 31:4274–4280
  78. Mishra S, Mohanty AK, Drzal LT, Misra M, Hinrichsen G (2004) A review on pineapple leaf fibers, sisal fibers and their biocomposites. *Macromol Mater Eng* 289:955–974
  79. Zhou Q, Zhang L, Zhang M, Wang B, Wang S (2003) Miscibility, free volume behavior and properties of blends from cellulose acetate and castor oil-based polyurethane. *Polymer* 44:1733–1739
  80. Yussuf A, Massoumi I, Hassan A (2010) Comparison of polylactic acid/kenaf and polylactic acid/rice husk composites: the influence of the natural fibers on the mechanical, thermal and biodegradability properties. *J Polym Environ* 18:422–429
  81. Zhao Q, Tao J, Yam RC, Mok AC, Li RK, Song C (2008) Biodegradation behavior of polycaprolactone/rice husk ecocomposites in simulated soil medium. *Polym Degrad Stab* 93:1571–1576

82. Martin AR, Martins MA, da Silva OR, Mattoso LH (2010) Studies on the thermal properties of sisal fiber and its constituents. *Thermo Acta* 506:14–19
83. Marichelvam M, Jawaid M, Asim M (2019) Corn and rice starch-based bio-plastics as alternative packaging materials. *Fiber* 7:32
84. Junior AC, Barreto A, Rosa D, Maia F, Lomonaco D, Mazzetto S (2015) Thermal and mechanical properties of biocomposites based on a cashew nut shell liquid matrix reinforced with bamboo fibers. *J Compos Mater* 49:2203–2215
85. Rout R, Jena S, Das S (2003) Spectral and thermal studies of biomass cured phenolic resin polymers. *Biomass Bioenergy* 25:329–334
86. Silva ALd, Silva LRRd, Camargo IdA, Agostini DLdS, Rosa DdS, Oliveira DLVd, Fachine PBA, Mazzetto SE (2016) Cardanol-based thermoset plastic reinforced by sponge gourd fibers (*Luffa cylindrica*). *Polímeros* 26:21–29
87. Modibbo U, Aliyu B, Nkafamiya I, Manji A (2007) The effect of moisture imbibition on cellulosic bast fibers as industrial raw materials. *Int J Phys Sci* 2:163–168
88. Szczesniak L, Rachocki A, Tritt-Goc J (2008) Glass transition temperature and thermal decomposition of cellulose powder. *Cellulose* 15:445–451
89. Thakur V, Singha A, Thakur M (2012) Biopolymers based green composites: mechanical, thermal and physico-chemical characterization. *J Polym Environ* 20:412–421
90. Fortunati E, Armentano I, Iannoni A, Kenny J (2010) Development and thermal behaviour of ternary PLA matrix composites. *Polym Degrad Stab* 95:2200–2206
91. Nasir M, Gupta A, Beg M, Chua GK, Jawaid M, Kumar A, Khan TA (2013) Fabricating eco-friendly binderless fiberboard from laccase-treated rubber wood fiber. *BioResources* 8:3599–3608
92. Quintana E, Valls C, Barneto AG, Vidal T, Ariza J, Roncero MB (2015) Studying the effects of laccase treatment in a softwood dissolving pulp: cellulose reactivity and crystallinity. *Carbohydr Polym* 119:53–61
93. Zhu Z, Wu H, Ye C, Fu W (2017) Enhancement on mechanical and thermal properties of PLA biocomposites due to the addition of hybrid sisal fibers. *J Nat Fiber* 14:875–886
94. Qian S, Sheng K, Yao W, Yu H (2016) Poly (lactic acid) biocomposites reinforced with ultrafine bamboo-char: morphology, mechanical, thermal, and water absorption properties. *J Appl Polym Sci* 133:43425
95. Ahmad E, Luyt A (2012) Morphology, thermal, and dynamic mechanical properties of poly (lactic acid)/sisal whisker nanocomposites. *Polym Compos* 33:1025–1032
96. Torres-Tello EV, Robledo-Ortiz JR, González-García Y, Pérez-Fonseca AA, Jasso-Gastinel CF, Mendizábal E (2017) Effect of agave fiber content in the thermal and mechanical properties of green composites based on polyhydroxybutyrate or poly (hydroxybutyrate-co-hydroxyvalerate). *Ind Crop Prod* 99:117–125
97. Bhardwaj R, Mohanty AK, Drzal L, Pourboghra F, Misra M (2006) Renewable resource-based green composites from recycled cellulose fiber and poly (3-hydroxybutyrate-co-3-hydroxyvalerate) bioplastic. *Biomacromol* 7:2044–2051
98. Espinach F, Boufi S, Delgado-Aguilar M, Julián E, Mutjé P, Méndez J (2018) Composites from poly (lactic acid) and bleached chemical fibers: thermal properties. *Compos B* 134:169–176
99. Reixach R, Puig J, Méndez JA, Gironès J, Espinach FX, Arbat G, Mutjé P (2015) Orange wood fiber reinforced polypropylene composites: thermal properties. *BioResources* 10:2156–2166
100. Shibata S, Cao Y, Fukumoto I (2008) Flexural modulus of the unidirectional and random composites made from biodegradable resin and bamboo and kenaf fibers. *Compos A* 39:640–646
101. Asim M, Paridah M, Saba N, Jawaid M, Allothman OY, Nasir M, Almutairi Z (2018) Thermal, physical properties and flammability of silane treated kenaf/pineapple leaf fibers phenolic hybrid composites. *Compos Struct* 202:1330–1338
102. Jawaid M, Khalil HA, Alattas OS (2012) Woven hybrid biocomposites: dynamic mechanical and thermal properties. *Compos A* 43:288–293
103. Ray D, Sarkar B, Das S, Rana A (2002) Dynamic mechanical and thermal analysis of vinyl ester-resin-matrix composites reinforced with untreated and alkali-treated jute fibers. *Compos Sci Technol* 62:911–917
104. Panthapulakkal S, Sain M (2007) Injection-molded short hemp fiber/glass fiber-reinforced polypropylene hybrid composites: mechanical, water absorption and thermal properties. *J Appl Polym Sci* 103:2432–2441
105. Braga R, Magalhaes P Jr (2015) Analysis of the mechanical and thermal properties of jute and glass fiber as reinforcement epoxy hybrid composites. *Mater Sci Eng C* 56:269–273
106. Jamshaid H, Mishra R, Militky J, Pechociakova M, Noman MT (2016) Mechanical, thermal and interfacial properties of green composites from basalt and hybrid woven fabrics. *Fiber Polym* 17:1675–1686
107. Boopalan M, Niranjanaa M, Umapathy M (2013) Study on the mechanical properties and thermal properties of jute and banana fiber reinforced epoxy hybrid composites. *Compos B* 51:54–57
108. Jawaid M, Khalil HA, Hassan A, Dungani R, Hadiyane A (2013) Effect of jute fiber loading on tensile and dynamic mechanical properties of oil palm-epoxy composites. *Compos B* 45:619–624
109. Threepopnatkul P, Kaerkitcha N, Athipongarporn N (2009) Effect of surface treatment on performance of pineapple leaf fiber-polycarbonate composites. *Compos B* 40:628–632
110. Huda M, Drzal L, Mohanty A, Misra M (2007) The effect of silane treated-and-untreated-talc on the mechanical and physico-mechanical properties of poly (lactic acid)/newspaper fibers/talc hybrid composites. *Compos B* 38:367–379
111. Nayak SK, Mohanty S (2010) Sisal glass fiber reinforced PP hybrid composites: effect of MAPP on the dynamic mechanical and thermal properties. *J Reinf Plast Compos* 29:1551–1568
112. Jawaid M, Allothman OY, Saba N, Tahir PM, Khalil HA (2015) Effect of fibers treatment on dynamic mechanical and thermal properties of epoxy hybrid composites. *Polym Compos* 36:1669–1674
113. Arrakhiz F, Elachaby M, Bouhfid R, Vaudreuil S, Essassi M, Qaiss A (2012) Mechanical and thermal properties of polypropylene reinforced with Alfa fiber under different chemical treatment. *Mater Des* 35:318–322
114. Nayak SK, Mohanty S, Samal SK (2009) Influence of short bamboo/glass fiber on the thermal, dynamic mechanical and rheological properties of polypropylene hybrid composites. *Mater Sci Eng A* 523:32–38
115. Samal SK, Mohanty S, Nayak SK (2009) Banana/glass fiber-reinforced polypropylene hybrid composites: fabrication and performance evaluation. *Polym Plast Technol Eng* 48:397–414
116. Bakar NA, Chee CY, Abdullah LC, Ratnam CT, Ibrahim NA (2015) Thermal and dynamic mechanical properties of grafted kenaf filled poly (vinyl chloride)/ethylene vinyl acetate composites. *Mater Des* 65:204–211
117. Ibrahim NA, Yunus WMZW, Abu-Ilaiwi FA, Rahman MZA, Bin Ahmad M, Dahlan KZM (2003) Graft copolymerization of methyl methacrylate onto oil palm empty fruit bunch fiber using  $H_2O_2/Fe^{2+}$  as an initiator. *J Appl Polym Sci* 89:2233–2238
118. Atiqah A, Jawaid M, Sapuan S, Ishak M, Allothman OY (2018) Thermal properties of sugar palm/glass fiber reinforced thermoplastic polyurethane hybrid composites. *Compos Struct* 202:954–958
119. Kc B, Tjong J, Jaffer S, Sain M (2018) Thermal and dimensional stability of injection-molded sisal-glass fiber hybrid PP biocomposites. *J Polym Environ* 26:1279–1289



120. Idicula M, Neelakantan N, Oommen Z, Joseph K, Thomas S (2005) A study of the mechanical properties of randomly oriented short banana and sisal hybrid fiber reinforced polyester composites. *J Appl Polym Sci* 96:1699–1709
121. Ademuwagun A, Myers J (2014) Biobased fillers for polypropylene for interior application. *SAE Technical Paper*
122. Norberg I (2012) Carbon fibers from kraft lignin. KTH Royal Institute of Technology, Stockholm
123. Birat K, Panthapulakkal S, Kronka A, Agnelli IAM, Tjong I, Sain M (2015) Hybrid biocomposites with enhanced thermal and mechanical properties for structural applications. *J Appl Polym Sci* 132:42452
124. El-Shekeil Y, Sapuan S, Jawaid M, Al-Shuja'a O (2014) Influence of fiber content on mechanical, morphological and thermal properties of kenaf fibers reinforced poly (vinyl chloride)/thermoplastic polyurethane poly-blend composites. *Mater Des* 58:130–135
125. Jumaidin R, Sapuan SM, Jawaid M, Ishak MR, Sahari J (2017) Thermal, mechanical, and physical properties of seaweed/sugar palm fiber reinforced thermoplastic sugar palm Starch/Agar hybrid composites. *Int J Biol Macromol* 97:606–615
126. Sanyang ML, Sapuan SM, Jawaid M, Ishak MR, Sahari J (2015) Effect of plasticizer type and concentration on tensile, thermal and barrier properties of biodegradable films based on sugar palm (*Arenga pinnata*) starch. *Polymer* 7:1106–1124
127. Prachayawarakorn J, Chaiwatyothin S, Mueangta S, Hanchana A (2013) Effect of jute and kapok fibers on properties of thermoplastic cassava starch composites. *Mater Des* 47:309–315
128. Prachayawarakorn J, Limsiriwong N, Kongjindamunee R, Surakit S (2012) Effect of agar and cotton fiber on properties of thermoplastic waxy rice starch composites. *J Polym Environ* 20:88–95
129. Nascimento T, Calado V, Carvalho C (2012) Development and characterization of flexible film based on starch and passion fruit mesocarp flour with nanoparticles. *Food Res Int* 49:588–595
130. Sanchez-Silva L, López-González D, Garcia-Minguillan A, Valverde J (2013) Pyrolysis, combustion and gasification characteristics of *Nannochloropsis gaditana* microalgae. *Bioresour Technol* 130:321–331
131. Ross A, Jones J, Kubacki M, Bridgeman T (2008) Classification of macroalgae as fuel and its thermochemical behaviour. *Biore-sour Technol* 99:6494–6504
132. Hamid MRY, Ab Ghani MH, Ahmad S (2012) Effect of antioxidants and fire retardants as mineral fillers on the physical and mechanical properties of high loading hybrid biocomposites reinforced with rice husks and sawdust. *Ind Crop Prod* 40:96–102
133. Kord B (2011) Effect of calcium carbonate as mineral filler on the physical and mechanical properties of wood based composites. *World Appl Sci J* 13:129–132
134. Zhao Q, Zhang B, Quan H, Yam RC, Yuen RK, Li RK (2009) Flame retardancy of rice husk-filled high-density polyethylene ecocomposites. *Compos Sci Technol* 69:2675–2681
135. Siakeng R, Jawaid M, Ariffin H, Sapuan S (2019) Mechanical, dynamic, and thermomechanical properties of coir/pineapple leaf fiber reinforced polylactic acid hybrid biocomposites. *Polym Compos* 40:2000–2011
136. Sathishkumar T, Ja N, Satheeshkumar S (2014) Hybrid fiber reinforced polymer composites—a review. *J Reinf Plast Compos* 33:454–471
137. Siakeng R, Jawaid M, Ariffin H, Sapuan S (2018) Thermal properties of coir and pineapple leaf fiber reinforced polylactic acid hybrid composites. In: *IOP Conference Series: Mater Sci Eng* 2018, vol 1, IOP Publishing, p 012019
138. Jang JY, Jeong TK, Oh HJ, Youn JR, Song YS (2012) Thermal stability and flammability of coconut fiber reinforced poly (lactic acid) composites. *Compos B* 43:2434–2438
139. Siakeng MI, Asim M, Saba N, Sanjay MR, Siengchin S, Foud H (2020) Alkali treated coir/pineapple leaf fibers reinforced PLA hybrid composites: evaluation of mechanical, morphological, thermal and physical properties. *Express Polym Lett* (accepted)
140. Islam MS, Ramli IB, Hasan M, Islam MM, Islam KN, Hasan M, Harmaen AS (2017) Effect of kenaf and EFB fiber hybridization on physical and thermo-mechanical properties of PLA biocomposites. *Fiber Polym* 18:116–121
141. Asaithambi B, Ganesan GS, Ananda Kumar S (2017) Banana/sisal fibers reinforced poly (lactic acid) hybrid biocomposites; influence of chemical modification of BSF towards thermal properties. *Polym Compos* 38:1053–1062
142. Carrasco F, Pagès P, Gámez-Pérez J, Santana O, MasPOCH ML (2010) Processing of poly (lactic acid): characterization of chemical structure, thermal stability and mechanical properties. *Polym Degrad Stab* 95:116–125
143. Tee YB, Talib RA, Abdan K, Chin NL, Basha RK, Yunus KFM (2013) Thermally grafting aminosilane onto kenaf-derived cellulose and its influence on the thermal properties of poly (lactic acid) composites. *BioResources* 8:4468–4483
144. Zainudin E, Sapuan S, Abdan K, Mohamad M (2009) Thermal degradation of banana pseudo-stem filled unplasticized poly-vinyl chloride (UPVC) composites. *Mater Des* 30:557–562
145. Kim KW, Lee BH, Kim HJ, Sriroth K, Dorgan JR (2011) Thermal and mechanical properties of cassava and pineapple flours-filled PLA bio-composites. *J Therm Anal Calorim* 108:1131–1139
146. Almeida E, Frollini E, Castellan A, Coma V (2010) Chitosan, sisal cellulose, and biocomposite chitosan/sisal cellulose films prepared from thiourea/NaOH aqueous solution. *Carbohydr Polym* 80:655–664
147. Oliveira M, Furtado R, Bastos M, Leitão R, Benevides S, Muniz C, Cheng H, Biswas A (2018) Performance evaluation of cashew gum and gelatin blend for food packaging. *Food Packag Shelf* 17:57–64
148. Mohajer S, Rezaei M, Hosseini SF (2017) Physico-chemical and microstructural properties of fish gelatin/agar bio-based blend films. *Carbohydr Polym* 157:784–793
149. Tongdeesoontorn W, Mauer LJ, Wongruong S, Sriburi P, Rachtanapun P (2011) Effect of carboxymethyl cellulose concentration on physical properties of biodegradable cassava starch-based films. *Chem Cent J* 5:1–6
150. Qiao C, Ma X, Zhang J, Yao J (2017) Molecular interactions in gelatin/chitosan composite films. *Food Chem* 235:45–50
151. Wang X, Hu Y, Song L, Xing W, Lu H (2010) Thermal degradation behaviors of epoxy resin/POSS hybrids and phosphorus–silicon synergism of flame retardancy. *J Polym Sci Pol Phys* 48:693–705
152. Arshad M, Kaur M, Ullah A (2016) Green biocomposites from nanoengineered hybrid natural fiber and biopolymer. *ACS Sustain Chem Eng* 4:1785–1793
153. Saba N, Jawaid M, Asim M (2019) Nanocomposites with nanofibers and fillers from renewable resources. *Green Compos Automot Appl* 2019:145–170
154. Azeez AA, Rhee KY, Park SJ, Hui D (2013) Epoxy clay nanocomposites—processing, properties and applications: a review. *Compos B* 45:308–320
155. Kaymakci A, Gulec T, Hosseinihashemi SK, Ayrilmis N (2017) Physical, mechanical and thermal properties of wood/zeolite/plastic hybrid composites. *Maderas Cienc Tecnol* 19:339–348
156. Idumah CI, Hassan A (2017) Hibiscus cannabinus fiber/PP based nano-biocomposites reinforced with graphene nanoplatelets. *J Nat Fiber* 14:691–706
157. Sajna V, Mohanty S, Nayak SK (2017) A study on thermal degradation kinetics and flammability properties of poly (lactic

- acid)/banana fiber/nanoclay hybrid bionanocomposites. *Polym Compos* 38:2067–2079
158. Huda MS, Drzal LT, Mohanty AK, Misra M (2008) Effect of fiber surface-treatments on the properties of laminated biocomposites from poly (lactic acid) (PLA) and kenaf fibers. *Compos Sci Technol* 68:424–432
  159. Bikiaris D (2011) Can nanoparticles really enhance thermal stability of polymers? Part II: an overview on thermal decomposition of polycondensation polymers. *Thermochim Acta* 523:25–45
  160. Qian S, Sheng K (2017) PLA toughened by bamboo cellulose nanowhiskers: role of silane compatibilization on the PLA bionanocomposite properties. *Compos Sci Technol* 148:59–69
  161. Sun P, Liu G, Lv D, Dong X, Wu J, Wang D (2015) Effective activation of halloysite nanotubes by piranha solution for amine modification via silane coupling chemistry. *RSC Adv* 5:52916–52925
  162. Saini S, Belgacem MN, Salon MCB, Bras J (2016) Non leaching biomimetic antimicrobial surfaces via surface functionalisation of cellulose nanofibers with aminosilane. *Cellulose* 23:795–810
  163. Gwon JG, Cho HJ, Chun SJ, Lee S, Wu Q, Lee SY (2016) Physicochemical, optical and mechanical properties of poly (lactic acid) nanocomposites filled with toluene diisocyanate grafted cellulose nanocrystals. *RSC Adv* 6:9438–9445
  164. Adel A, El-Shafei A, Ibrahim A, Al-Shemy M (2018) Extraction of oxidized nanocellulose from date palm (*Phoenix Dactylifera* L.) sheath fibers: Influence of CI and CH polymorphs on the properties of chitosan/bionanocomposite films. *Ind Crop Prod* 124:155–165
  165. Choo K, Ching YC, Chuah CH, Julai S, Liou NS (2016) Preparation and characterization of polyvinyl alcohol-chitosan composite films reinforced with cellulose nanofiber. *Material* 9:644
  166. Jafari M, Davachi SM, Mohammadi-Rovshandeh J, Poursmaeel-Selakjani P (2018) Preparation and characterization of bionanocomposites based on benzylated wheat straw and nanoclay. *J Polym Environ* 26:913–925
  167. Han R, Zhang L, Song C, Zhang M, Zhu H, Zhang L (2010) Characterization of modified wheat straw, kinetic and equilibrium study about copper ion and methylene blue adsorption in batch mode. *Carbohydr Polym* 79:1140–1149
  168. Di Y, Iannace S, Di Maio E, Nicolais L (2003) Nanocomposites by melt intercalation based on polycaprolactone and organoclay. *J Polym Sci Pol Phys* 41:670–678
  169. Seyfi J, Hejazi I, Mohamad Sadeghi GM, Davachi SM, Ghanbar S (2012) Thermal degradation and crystallization behavior of blend-based nanocomposites: role of clay network formation. *J Appl Polym Sci* 123:2492–2499
  170. Montes S, Etxeberria A, Mocholi V, Rekondo A, Grande H, Labidi J (2018) Effect of combining cellulose nanocrystals and graphene nanoplatelets on the properties of poly (lactic acid) based films. *Express Polym Lett* 12:543–555
  171. Saeidlou S, Huneault MA, Li H, Park CB (2012) Poly (lactic acid) crystallization. *Prog Polym Sci* 37:1657–1677
  172. Monteiro SN, Calado V, Rodriguez RJ, Margem FM (2012) Thermogravimetric stability of polymer composites reinforced with less common lignocellulosic fibers—an overview. *J Mater Res Technol* 1:117–126
  173. Dorez G, Taguet A, Ferry L, Lopez-Cuesta J (2013) Thermal and fire behavior of natural fibers/PBS biocomposites. *Polym Degrad Stab* 98:87–95
  174. Indran S, Raj RE (2015) Characterization of new natural cellulose fiber from *Cissus quadrangularis* stem. *Carbohydr Polym* 117:392–399
  175. Asim M, Abdan K, Jawaid M, Nasir M, Dashtizadeh Z, Ishak M, Hoque ME (2015) A review on pineapple leaves fiber and its composites. *Int J Polym Sci* 2015:1–16
  176. Álvarez A, Pizarro C, García R, Bueno J, Lavín A (2016) Determination of kinetic parameters for biomass combustion. *Biore-sour Technol* 216:36–43
  177. Azwa Z, Yousif B (2013) Thermal degradation study of kenaf fiber/epoxy composites using thermo gravimetric analysis. In: *Proceedings of the 3rd Malaysian Postgraduate Conference (MPC 2013)*, 2013. Education Malaysia, pp 256–264
  178. Asim M, Jawaid M, Paridah MT, Nasir M (2019) Thermo-gravimetric analysis of various ratio of blended phenolic and epoxy composites. *IJHTEE* 9:5435–5439
  179. Rojo E, Alonso MV, Oliet M, Del Saz-Orozco B, Rodriguez F (2015) Effect of fiber loading on the properties of treated cellulose fiber-reinforced phenolic composites. *Compos B* 68:185–192
  180. Del Saz-Orozco B, Alonso MV, Oliet M, Domínguez JC, Rodríguez F (2015) Mechanical, thermal and morphological characterization of cellulose fiber-reinforced phenolic foams. *Compos B* 75:367–372
  181. Singha A, Thakur VK (2008) Mechanical, morphological and thermal properties of pine needle-reinforced polymer composites. *Int J Polym Mater* 58:21–31
  182. Mehta G, Drzal LT, Mohanty AK, Misra M (2006) Effect of fiber surface treatment on the properties of biocomposites from nonwoven industrial hemp fiber mats and unsaturated polyester resin. *J Appl Polym Sci* 99:1055–1068
  183. Dhakal H, Zhang Z, Bennett N (2012) Influence of fiber treatment and glass fiber hybridisation on thermal degradation and surface energy characteristics of hemp/unsaturated polyester composites. *Compos B* 43:2757–2761
  184. Nadlene R, Sapuan S, Jawaid M, Ishak M, Yusriah L (2018) The effects of chemical treatment on the structural and thermal, physical, and mechanical and morphological properties of roselle fiber-reinforced vinyl ester composites. *Polym Compos* 39:274–287
  185. Shahroze RM, Ishak MR, Salit MS, Leman Z, Chandrasekar M, Munawar NS, Asim M (2019) Sugar palm fiber/polyester nanocomposites: influence of adding nanoclay fillers on thermal, dynamic mechanical, and physical properties. *J Vinyl Addit Technol*. <https://doi.org/10.1002/vnl.21736>
  186. Du Y, Wu T, Yan N, Kortschot MT, Farnood R (2013) Pulp fiber-reinforced thermoset polymer composites: effects of the pulp fibers and polymer. *Compos B* 48:10–17
  187. Elkhaoulani A, Arrakhiz F, Benmoussa K, Bouhfid R, Qaiss A (2013) Mechanical and thermal properties of polymer composite based on natural fibers: moroccan hemp fibers/polypropylene. *Mater Des* 49:203–208
  188. Essabir H, Nekhlaoui S, Malha M, Bensalah M, Arrakhiz F, Qaiss A, Bouhfid R (2013) Bio-composites based on polypropylene reinforced with almond shells particles: mechanical and thermal properties. *Mater Des* 51:225–230
  189. El Mechtali FZ, Essabir H, Nekhlaoui S, Bensalah MO, Jawaid M, Bouhfid R, Qaiss A (2015) Mechanical and thermal properties of polypropylene reinforced with almond shells particles: Impact of chemical treatments. *J Bionic Eng* 12:483–494
  190. Radzi A, Sapuan S, Jawaid M, Mansor M (2017) Influence of fiber contents on mechanical and thermal properties of roselle fiber reinforced polyurethane composites. *Fiber Polym* 18:1353–1358
  191. Sreenivasan V, Rajini N, Alavudeen A, Arumugaprabu V (2015) Dynamic mechanical and thermo-gravimetric analysis of *Sansevieria cylindrica*/polyester composite: effect of fiber length, fiber loading and chemical treatment. *Compos B* 69:76–86



192. Asim M, Saba N, Jawaid M, Nasir M, Pervaiz M, Alothman OY (2018) A review on phenolic resin and its composites. *Curr Anal Chem* 14:185–197
193. Lee SM, Cho D, Park WH, Lee SG, Han SO, Drzal LT (2005) Novel silk/poly (butylene succinate) biocomposites: the effect of short fiber content on their mechanical and thermal properties. *Compos Sci Technol* 65:647–657
194. Nam TH, Ogihara S, Nakatani H, Kobayashi S, Song JI (2012) Mechanical and thermal properties and water absorption of jute fiber reinforced poly (butylene succinate) biodegradable composites. *Adv Compos Mater* 21:241–258
195. Srinivasan V, Boopathy SR, Sangeetha D, Ramnath BV (2014) Evaluation of mechanical and thermal properties of banana–flax based natural fiber composite. *Mater Des* 60:620–627
196. AlMaadeed MA, Kahraman R, Khanam PN, Madi N (2012) Date palm wood flour/glass fiber reinforced hybrid composites of recycled polypropylene: mechanical and thermal properties. *Mater Des* 42:289–294
197. Ying-Chen Z, Hong-Yan W, Yi-Ping Q (2010) Morphology and properties of hybrid composites based on polypropylene/poly(lactic acid) blend and bamboo fiber. *Bioresour Technol* 101:7944–7950
198. Park HM, Lee WK, Park CY, Cho WJ, Ha CS (2003) Environmentally friendly polymer hybrids: part I mechanical, thermal, and barrier properties of thermoplastic starch/clay nanocomposites. *J Mater Sci* 38:909–915